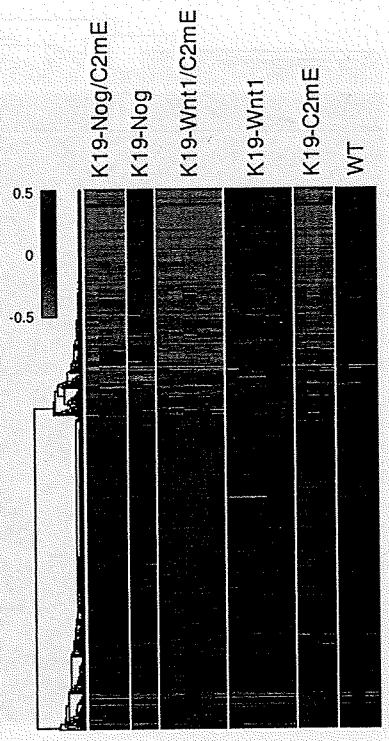

Figure 1
Genome-scale expression pattern of transgenic mice showing major changes are caused by PGE_2 induction. Clustered in rows are 5,440 probe sets selected by fold change threshold of 2 or greater to the average of wild-type and a ratio p-value of 0.01 or less, and columns are mouse gastric samples grouped by genotype. Genotypes are shown on the top of the heatmap. The red-green color scale represents log10 ratio to the average of wild-type samples, as shown in a color bar on top left: red color indicates the gene is up-regulated in the sample, and green indicates down-regulated. WT: wild-type.

inflammatory response were significantly condensed with the p-value of 1.5×10^{-21} and 4.2×10^{-13}, respectively, in the gene set changed by the C2mE induction.

Classification of mouse tumor models under a human gastric cancer subtype

In order to confirm that the mouse gastric tumor models are similar to human gastric cancer, the expression profiles were compared with those of human cancer samples. First, gene expression data of human breast, lung, colon, and gastric tumors were collected from public domain. To estimate similarity between the mouse gastric tumors and the four types of human cancers, supervised classification of principal component analysis (PCA) was conducted using 1,925 genes which were changed more than two-fold in more than 50 samples of all human samples. The

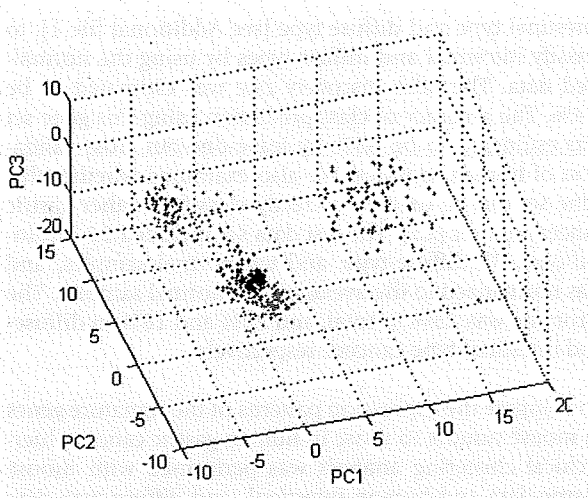

Figure 2
Overall expression changes in gastric tumors of C2mE-related transgenic mice are most similar to those in human gastric cancers. *K19-C2mE*, *K19-Wnt1/C2mE*, and *K19-Nog/C2mE* mouse gastric tumors and human gastric (diffuse, intestinal, and mixed type), colon, breast, and lung cancers were plotted by principal component 1 to 3 (PC1 to PC3) calculated using 1,925 genes which were changed by more than two-fold in more than 50 samples of all. The cumulative contribution of the three components was 32%. Dots shown in blue: human gastric cancers; cyan: human colon cancers; red: human lung cancers; green: human breast cancers; magenta: mouse model tumors.

PCA with the selected genes found that mouse gastric samples from C2mE-related mice were most closely clustered to human gastric cancers among the four tissues examined, indicating the global expression changes in the gastric tumors of the transgenic mice resembled those in human gastric cancers (Figure 2).

Next, in order to examine which subtype of gastric cancer shows cross-species similarity, the mouse tumors were compared with human gastric intestinal-type and diffuse-type cancers on the basis of their expression profiles. Previous expression profiling studies of human gastric tumor samples have identified gene signatures that classify the two types. Intestinal and diffuse types are the two major types of cancer classified on the basis of microscopic morphology [1]. Boussioutas *et al.* [15] showed that proliferation genes were over-expressed in intestinal-type tumors than in diffuse-type tumors; in contrast, extracellular matrix protein genes were up-regulated in diffuse-type compared with intestinal-type tumors. In order to determine which type of human gastric cancer the mouse models are more similar to, we normalized the human data [20] to the average of normal samples, and selected 122 genes which were changed in the opposite direction in

intestinal type and diffuse type [see Additional file 1], to classify intestinal and diffuse types by using the normalized data. The false discovery rate was estimated to be 2.4%. The accuracy of class prediction using this gene set was estimated to be 85% by leave-one-out cross-validation of human samples. We also examined whether this gene set can be used to correctly classify another gastric cancer data set [15]. The test data set included 22 intestinal-type, 35 diffuse-type, and ten normal samples, and was normalized to the average of all normal samples. The error rate was 25% in total, and 29% and 18% in diffuse- and intestinal-type cancers, respectively.

To compare the expression patterns of the signature genes in mouse tumors to those in human gastric cancers, hierarchical clustering analysis was performed with mouse gastric data and human intestinal- and diffuse-type data sets. The expression pattern of our modified signature genes for distinguishing intestinal- and diffuse-type gastric cancers revealed that the gastric tumors from C2mE-related transgenic mice were more similar to intestinal-type human gastric cancers than to diffuse-type human gastric cancers (Figure 3). By linear discriminant analysis, all C2mE-related gastric tumors except one K19-Wnt1/C2mE sample were classified as intestinal-type tumors.

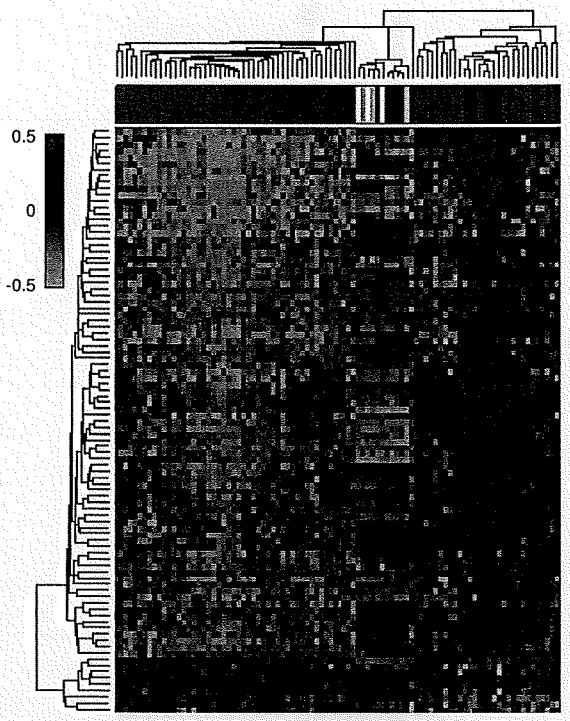

Figure 3
Expression profiles of C2mE-related gastric tumors are clustered to human intestinal-type gastric cancers. Clustered in rows are 93 genes which met p-value less than 0.001 and opposite change direction between intestinal-type and diffuse-type human gastric cancers, and clustered in columns are human and mouse gastric tumors. As a distance measure, cosine correlation was used. Linkage method for clustering was average linkage. Samples shown in red: human intestinal type gastric cancers; blue: human diffuse type; yellow: *K19-C2mE* mice; magenta: *K19-Wnt1/C2mE*: cyan: *K19-Nog/C2mE*. The red-green color scale represents log10 ratio to the average of wild-type or normal samples, as shown in a color bar on top left.

Expression pattern of the genes frequently deregulated in human gastric cancer in a subtype specific manner

It is known that amplification or overexpression of some genes are found in a subtype-specific manner. E-cadherin gene mutations or loss are specifically found in diffuse-type gastric cancer [11,12]. In contrast, amplification of *ErbB2* gene is observed only in intestinal type, and not reported in diffuse type [6,7]. LOH of deleted in colorectal carcinoma (*DCC*) is predominantly observed in about half of intestinal-type [21,22]. Expression levels of the three genes were compared between mice and human gastric cancer types (Table 1). *CDH1* expression was significantly decreased in human diffuse type but not in intestinal type as expected. In the three transgenic mice, *Cdh1* gene was not decreased in any of transgenic mice compared with wild-type, inferring that one of the most characteristic changes in human diffuse type gastric cancer was not observed in the mouse models. Up-regulation of *ErbB2* was observed in human intestinal-type microarray data, and also in our mouse data. *DCC* expression was reduced in human intestinal-type as expected, while the reduction of the gene was observed in the mice model, especially in *K19-Wnt1/C2mE* mice. The expressions of the three genes defining the tissue-type of the human gastric cancer also support the idea that the mouse models are more similar to intestinal-type human cancer.

Difference among PGE_2 pathway-activated mouse models

Tumors from three mouse models with PGE_2 pathway activation show different histology. *K19-C2mE* develops hyperplasia with macrophage infiltration, whereas *K19-Wnt1/C2mE* develops dysplasia [17,18]. *K19-Nog/C2mE* develops hamartoma similar to human juvenile polyposis [19]. We next attempted to identify differentially expressed genes among the three mouse models which allowed us to assess the best-fit model among the three to study gastric intestinal-type cancer. With ANOVA p-value threshold of 0.001, we selected 155 genes which were differently regulated among the three groups. Few of these genes showed expression changes in the same direction between *K19-Wnt1/C2mE* and *K19-Nog/C2mE* (Figure 4). Wnt pathway genes *Porcn*, an acyltransferase required for Wnt protein secretion, β-catenin (*Ctnnb1*), and *Tcfe2a* (*TCF3* in human) were overexpressed in *K19-Wnt1/C2mE*

Table 1: Expression changes of subtype-specific genes in mouse and human gastric tumors.

	Mouse			Human	
	C2mE	Wnt1/C2mE	Nog/C2mE	Diffuse	Intestinal
CDH1	1.13*	1.00	1.10	0.43*	1.09
ErbB2	1.37*	1.43*	1.25*	0.92	1.37*
DCC	0.91	0.85*	0.94	0.98	0.71*

Expression values are shown in average log ratios (base 10) to wild-type or normal samples. Asterisk indicates t-test p-value < 0.05.

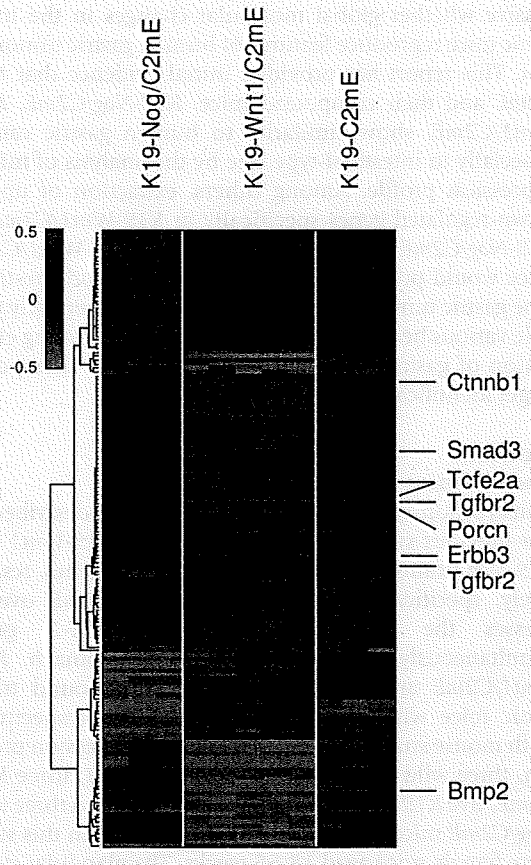

Figure 4
Wnt/β-catenin regulatory genes are up-regulated in Wnt1/C2mE mice. Clustered in rows are 155 probe sets which were differently regulated among three genotypes, *K19-C2mE*, *K19-Wnt1/C2mE*, and *K19-Nog/C2mE*, using ANOVA p-value threshold 0.001. Columns show mouse gastric sample grouped by genotype and genotypes are shown on top of the heatmap. Color scale is same as in Figure 1.

mice, but not in *K19-Nog/C2mE* (Figure 4). TGF-β/BMP pathway genes *Smad3* and *Tgfbr2* were also up-regulated and *Bmp2* was down-regulated in *K19-Wnt1/C2mE* but not in *K19-Nog/C2mE*.

In *K19-Nog/C2mE* mice, some genes which promote tumorigenesis were up- or down-regulated, although they have not been reported in the downstream of BMP pathway. *ROCKII* was specifically up-regulated in *K19-Nog/C2mE*, and its overexpression is associated with progression in several types of cancers via modulating actin cytoskeleton organization. Down-regulated genes include *RAMP2* and *PPARGC1A*, and their inactivation or underexpression was shown to contribute to lung cancer and hepatoma development respectively.

Since deregulation of Wnt pathway including *APC* or *CTNNB1* mutation have been more frequently observed in intestinal-type compared with diffuse-type [23,24], the results indicated that *K19-Wnt1/C2mE* could offer a model that best-fits intestinal-type tumors among the three C2mE-related mice.

Discussion

The present study indicated that human intestinal-type gastric cancers exhibited significant similarity to C2mE-related mice, especially to *K19-Wnt1/C2mE* mice by global expression profiling. The prediction of similar tumor type by global expression profile is consistent with the phenotypes of the transgenic mice. Accumulating evidence has indicated that inflammation level which is caused by the up-regulated expression/activity of *COX-2* and *mPGES-1* is severer in intestinal-type gastric cancer compared with diffuse-type one, although both types of tumors are related to *Helicobacter pylori* that are known to induce inflammation to the infected site [14,25-28]. This knowledge supports our observation that gastric tumors in C2mE-related mice in which PGE_2 pathway is activated exhibit similarity to intestinal-type gastric tumors. In addition, activating and inactivating mutations in *CTNNB1* and *APC* are more frequently observed in intestinal-type cancer. No *APC* LOH/mutation were observed in diffuse-type gastric cancer, whereas 60% were found in intestinal-type one [24,29,30]. Mutation in *CTNNB1* was

predominantly observed in intestinal-type one [13]. This is also concordant with our previous finding that *K19-Wnt1/C2mE* mice which only develop adenocarcinoma among the three C2mE-related mice activate down stream genes of Wnt/β-catenin pathway.

Usually, several types of transgenic mice for one tumor type are required to examine similarity in global expression profiling between mice tumor models and human ones, since the genes which were up- or down-regulated in each mice model were extracted compared to the average of all the examined tumor samples. With this approach, Lee *et al.* [31] analyzed gene expression data of seven mouse hepatocellular carcinomas (HCCs) including five GEMs with human HCCs to identify models that recapitulate human cancer or a type of human cancer, and found that some subclasses of human HCC mimic mice models in expression pattern. Hershkowitz *et al.* [32] also used the same normalization method, and found that characteristic expression patterns observed in human breast tumors were conserved in 13 mouse breast tumor models. Since the available data of expression profile for mouse gastric tumors are limited to our *K19-C2mE* and its compound mice, we took different strategy to assess the similarity of gastric tumors between the two species. Instead of using average of all samples in the dataset as a reference to calculate expression ratios, we normalized the mouse gastric data to average of wild-type samples. To compare our mice expression profiles with those of human gastric cancers, the gene signature to classify human intestinal- and diffuse-type gastric cancers was also modified from original one by normalizing the expression data to the average of normal gastric samples. This has allowed us to reveal that C2mE-related transgenic mice resemble human intestinal-type gastric tumors in expression profiling.

Comparison of gene expressions between mouse models showed that simultaneous induction of Wnt1 and PGE_2 deregulated not only gene expression of *Ctnnb1* and *Porcn* in Wnt signaling but also *Smad3* and *Tgfbr2* in TGF-β/BMP signaling. Given the crosstalk between TGF-β/BMP and Wnt pathways has been reported in multiple previous studies, the deregulated expression of the genes in the additional signaling pathways could be explained by positive and negative feedback to the pathways from the up-regulated Wnt signaling. For example, BMP signaling is known to suppress β-catenin activity in intestinal stem cells [33]. BMP signaling could be repressed in *K19-Wnt1/C2mE*, because *Bmp2* expression was significantly down-regulated. Increase in *Smad3* and *Tgfbr2* might be resulted from the negative feedback by BMP signaling suppression, as demonstrated in a study on TGF-β induced fibrosis [34]. In contrast to *K19-Wnt1/C2mE* transgenic mice, expression changes of the Wnt pathway genes were not observed in *K19-C2mE* and *K19-Nog/C2mE* mice. It would be of great interest to further analyze the crosstalk of signaling pathways in the compound transgenic mice.

Conclusions

Genetically engineered mouse (GEM) models provide useful tools to study mechanism of tumorigenesis, to validate a new target for drug development, and to find biomarkers. Advances in genetic engineering have allowed us to develop a variety of transgenic or knockout models of human diseases. The main question on using GEMs as disease models is whether the model recapitulates the human disease. We previously developed several gastric tumor transgenic mice in which prostaglandin E_2 pathway is activated. Although we conducted detailed histological analysis with the transgenic mice, it remained elusive whether global molecular changes in the transgenic mice reproduce features of human gastric tumors or not. This report has provided initial evidence that *K19-C2mE* and their compound mice, *K19-Nog/C2mE*, *K19-Wnt1/C2mE*, show similarity to human gastric cancer, especially to intestinal-type one by the analysis of mRNA expression profile. Among others, extraction of up- or down-regulated genes specifically in *K19-Wnt1/C2mE* or *K19-Nog/C2mE* respectively inferred that *K19-Wnt1/C2mE* mice would provide best-fit mouse model for intestinal-type gastric tumors. These findings would potentially provide various benefits in our future studies including elucidation of gastric tumorigenesis and optimal therapeutic target identification.

Methods

Stomach tissue samples

Construction of transgenic mice have been described in our previous studies [17-19]. Briefly, the *K19-Wnt1* and *K19-Nog* strains overexpress *Wnt1* and *Nog* genes, respectively, specifically in the stomach. *K19-C2mE* overexpresses the *mPGES-1* gene and *COX-2* genes simultaneously and specifically in the stomach. *K19-Wnt1/C2mE* and *K19-Nog/C2mE* are compound transgenic mice with *K19-Wnt1* and *K19-Nog*, respectively; both mouse strains have *K19-C2mE*. For expression profiling, three wild-type C57BL/6, five *K19-Wnt1*, three *K19-C2mE*, five *K19-Wnt1/C2mE*, two *K19-Nog*, and three *K19-Nog/C2mE* mice were used. All animals used in this study were female mice aged 18-65 weeks. The glandular stomach of each mouse was cut for microarray analysis. All animal studies were carried out in accordance with good animal practice as defined by the Institutional Animal Care and Use Committee (IACUC).

Microarrays

GeneChip Mouse Genome 430 2.0 Arrays (Affymetrix, Inc.) were used to monitor the expression profiles of the gastric samples. Total RNA was prepared using the RNeasy Mini Kit (QIAGEN) after treatment with TRIzol (Invitro-

gen Corp.), and labeled cRNA was prepared using standard Affymetrix protocols. The signal intensities of the probe sets were normalized by the Affymetrix Power Tools RMA method implemented in Resolver software (Rosetta Biosoftware), and log ratio values to the average of wild-type samples were calculated for each sample by using Resolver. All the microarray data were deposited at Gene Expression Omnibus (GEO) under dataset accession no. GSE16902 [35].

Public human microarray data

Human gastric cancer [20] and breast cancer [36] microarray data were retrieved from the online supplement in the Stanford Microarray Database [37]. The gastric cancer data includes 68 intestinal-type cancer, 13 diffuse-type cancer, and 15 normal gastric samples. The breast cancer data include 115 breast tumor and seven normal tissue samples. Human colon cancer data [38], including 100 colorectal cancer and five normal tissue samples, were retrieved from NCBI GEO under accession GSE5206. The Ann Arbor lung tumor dataset [39] including 86 lung adenocarcinomas and 10 non-neoplastic lung samples was obtained from the United States National Cancer Institute website [40]. Expression values were transformed to log10 (ratio to geometric averages of normal samples) in order to compare with mouse data.

Intestinal vs. diffuse type signature genes

Human gastric tumor data from Chen *et al.* [20] were used to develop an intestinal vs. diffuse type classifier. We selected genes that met the following criteria: (1) t-test p-value < 0.001 between the two groups, (2) opposite changes in the average expression of signature genes in intestinal-type tumors and that of signature genes in diffuse-type tumors. The false discovery rate was estimated by the Benjamini and Hochberg method [41]. The tumor classes of mouse and human samples were predicted by linear discriminant analysis using the signature score defined by the following formula:

Signature score = (Average log ratio of genes up-regulated in intestinal-type tumors and down-regulated in diffuse-type tumors) - (Average log ratio of genes down-regulated in intestinal-type tumors and up-regulated in diffuse-type tumors)

Combining mouse and human gene expression data

In order to combine mouse data with human gastric cancer microarray data, mouse and human data were re-ratioed to the geometric average of wild-type and normal samples, respectively. When there was more than one probe set for a gene in a microarray, the averaged expression ratios were used for the gene. Next, using only homologous genes that are represented in both arrays, we merged the mouse and human data sets into a single data set. The mouse microarray contains 45,037 probe sets, which correspond to 21,066 Entrez genes, and the human microarray contains 6,688 probes, which correspond to 4,463 Entrez genes. When they were merged, 4,094 homologous genes were identified.

Statistical analysis

The hypergeometric test for Gene Ontology enrichment was performed using the Gene Set Annotator developed by Rosetta Inpharmatics [42]. For the other statistical analyses in this study, the MATLAB software (MathWorks Inc.) was used.

Authors' contributions

MO and HK designed the research. HO constructed the transgenic animals and prepared the stomach tissue samples. HI analyzed the microarray data and wrote the manuscript. All authors read and approved the final manuscript.

Additional material

Additional file 1

A list of intestinal type vs. diffuse type signature genes. Sequence accession, gene symbol, and the average of log10 ratios in intestinal-type and in diffuse-type, respectively, are shown for each of the 122 cDNAs.
Click here for file
[http://www.biomedcentral.com/content/supplementary/1471-2164-10-615-S1.XLS]

Acknowledgements

The authors would like to thank Dr. Tsutomu Kobayashi for his assistance in the microarray experiment, and Dr. Shinji Mizuarai for his discussion and comments on the manuscript.

References

1. Lauren P: **The two histological main types of gastric carcinoma - diffuse and so-called intestinal-type carcinoma - An attempt at a histo-clinical classification.** *Acta Pathologica et Microbiologica Scandinavica* 1965, **64**:31-49.
2. Tahara E: **Genetic pathways of two types of gastric cancer.** *Iarc Sci Publ* 2004:327-349.
3. Vauhkonen M, Vauhkonen H, Sipponen P: **Pathology and molecular biology of gastric cancer.** *Best Practice & Research in Clinical Gastroenterology* 2006, **20**:651-674.
4. Yokota J, Yamamoto T, Miyajima N, Toyoshima K, Nomura N, Sakamoto H, Yoshida T, Terada M, Sugimura T: **Genetic alterations of the c-erbB-2 oncogene occur frequently in tubular adenocarcinoma of the stomach and are often accompanied by amplification of the v-erbA homologue.** *Oncogene* 1988, **2**:283-287.
5. Kameda T, Yasui W, Yoshida K, Tsujino T, Nakayama H, Ito M, Ito H, Tahara E: **Expression of *ERBB2* in Human Gastric Carcinomas: Relationship between $p185^{ERBB2}$ Expression and the Gene Amplification.** *Cancer Research* 1990, **50**:8002-8009.
6. Tsugawa K, Yonemura Y, Hirono Y, Fushida S, Kaji M, Miwa K, Miyazaki I, Yamamoto H: **Amplification of the c-met, c-erbB2 and epidermal growth factor receptor gene in human gastric cancers: Correlation to clinical features.** *Oncology* 1998, **55**:475-481.

7. Yonemura Y, Ninomiya I, Ohoyama S, Kimura H, Yamaguchi A, Fushida S, Kosaka T, Miwa K, Miyazaki I, Endou Y, Tanaka M, Sasaki T: **Expression of c-erbB-2 Oncoprotein in Gastric Carcinoma. Immunoreactivity for c-erbB-2 Protein is an Independent Indicator of Poor Short-Term Prognosis in Patients With Gastric Carcinoma.** *Cancer* 1991, **67**:2914-2918.
8. Mayer B, Johnson JP, Leitl F, Jauch KW, Heiss MM, Schildberg FW, Birchmeier W, Funke I: **E-Cadherin Expression in Primary and Metastatic Gastric Cancer: Down-Regulation Correlates with Cellular Dedifferentiation and Glandular Disintegration.** *Cancer Research* 1993, **53**:1690-1695.
9. Gabbert HE, Mueller W, Schneiders A, Meier S, Moll R, Birchmeier W, Hommel G: **Prognostic value of E-cadherin expression in 413 gastric carcinomas.** *International Journal of Cancer* 1996, **69**:184-189.
10. Ascano JJ, Frierson H, Moskaluk CA, Harper JC, Roviello F, Jackson CE, El Rifai W, Vindigni C, Tosi P, Powell SM: **Inactivation of the E-cadherin gene in sporadic diffuse-type gastric cancer.** *Modern Pathology* 2001, **14**:942-949.
11. Guilford P, Hopkins J, Harraway J, McLeod M, McLeod N, Harawira P, Taite H, Scoular R, Miller A, Reeve AE: **E-cadherin germline mutations in familial gastric cancer.** *Nature* 1998, **392**:402-405.
12. Berx G, Becker KF, Hofler H, van Roy F: **Mutations of the human E-cadherin (*CDH1*) gene.** *Human Mutation* 1998, **12**:226-237.
13. Ebert MPA, Fei G, Kahmann S, Muller O, Yu J, Sung JJY, Malfertheiner P: **Increased β-catenin mRNA levels and mutational alterations of the *APC* and β-catenin gene are present in intestinal-type gastric cancer.** *Carcinogenesis* 2002, **23**:87-91.
14. Saukkonen K, Nieminen O, van Rees B, Vilkki S, Harkonen M, Juhola M, Mecklin JP, Sipponen P, Ristimaki A: **Expression of cyclooxygenase-2 in dysplasia of the stomach and in intestinal-type gastric adenocarcinoma.** *Clinical Cancer Research* 2001, **7**:1923-1931.
15. Boussioutas A, Li H, Liu J, Waring P, Lade S, Holloway AJ, Taupin D, Gorringe K, Haviv I, Desmond PV, Bowtell DDL: **Distinctive patterns of gene expression in premalignant gastric mucosa and gastric cancer.** *Cancer Research* 2003, **63**:2569-2577.
16. Jinawath N, Furukawa Y, Hasegawa S, Li MH, Tsunoda T, Satoh S, Yamaguchi T, Imamura H, Inoue M, Shiozaki H, Nakamura Y: **Comparison of gene-expression profiles between diffuse- and intestinal-type gastric cancers using a genome-wide cDNA microarray.** *Oncogene* 2004, **23**:6830-6844.
17. Oshima H, Oshima M, Inaba K, Taketo MM: **Hyperplastic gastric tumors induced by activated macrophages in COX-2/mPGES-1 transgenic mice.** *EMBO Journal* 2004, **23**:1669-1678.
18. Oshima H, Matsunaga A, Fujimura T, Tsukamoto T, Taketo MM, Oshima M: **Carcinogenesis in mouse stomach by simultaneous activation of the Wnt signaling and prostaglandin E_2 pathway.** *Gastroenterology* 2006, **131**:1086-1095.
19. Oshima H, Itadani H, Kotani H, Taketo MM, Oshima M: **Induction of prostaglandin E_2 pathway promotes gastric hamartoma development with suppression of bone morphogenetic protein signaling.** *Cancer Research* 2009, **69**:2729-2733.
20. Chen X, Leung SY, Yuen ST, Chu KM, Ji JF, Li R, Chan ASY, Law S, Troyanskaya OG, Wong J, So S, Botstein D, Brown PO: **Variation in gene expression patterns in human gastric cancers.** *Molecular Biology of the Cell* 2003, **14**:3208-3215.
21. Sano T, Tsujino T, Yoshida K, Nakayama H, Haruma K, Ito H, Nakamura Y, Kajiyama G, Tahara E: **Frequent Loss of Heterozygosity on Chromosomes 1q, 5q, and 17p in Human Gastric Carcinomas.** *Cancer Research* 1991, **51**:2926-2931.
22. Uchino S, Tsuda H, Noguchi M, Yokota J, Terada M, Saito T, Kobayashi M, Sugimura T, Hirohashi S: **Frequent Loss of Heterozygosity at the *DCC* Locus in Gastric Cancer.** *Cancer Research* 1992, **52**:3099-3102.
23. Park WS, Oh RR, Park JY, Lee SH, Shin MS, Kim YS, Kim SY, Lee HK, Kim PJ, Oh ST, Yoo NJ, Lee JY: **Frequent Somatic Mutations of the β-catenin Gene in Intestinal-Type Gastric Cancer.** *Cancer Research* 1999, **59**:4257-4260.
24. Nakatsuru S, Yanagisawa A, Ichii S, Tahara E, Kato Y, Nakamura Y, Horii A: **Somatic mutation of the *APC* gene in gastric cancer: Frequent mutations in very well differentiated adenocarcinoma and signet-ring cell carcinoma.** *Human Molecular Genetics* 1992, **1**:559-563.
25. Parsonnet J, Vandersteen D, Goates J, Sibley RK, Pritikin J, Chang Y: ***Helicobacter pylori* Infection in Intestinal-Type and Diffuse-Type Gastric Adenocarcinomas.** *Journal of the National Cancer Institute* 1991, **83**:640-643.
26. Uemura N, Okamoto S, Yamamoto S, Matsumura N, Yamaguchi S, Yamakido M, Taniyama K, Sasaki N, Schlemper RJ: ***Helicobacter pylori* Infection and the Development of Gastric Cancer.** *New England Journal of Medicine* 2001, **345**:784-789.
27. Akhtar M, Cheng YL, Magno RM, Ashktorab H, Smoot DT, Meltzer SJ, Wilson KT: **Promoter Methylation Regulates *Helicobacter pylori*-stimulated Cyclooxygenase-2 Expression in Gastric Epithelial Cells.** *Cancer Research* 2001, **61**:2399-2403.
28. Yamagata R, Shimoyama T, Fukuda S, Yoshimura T, Tanaka M, Munakata A: **Cyclooxygenase-2 expression is increased in early intestinal-type gastric cancer and gastric mucosa with intestinal metaplasia.** *European Journal of Gastroenterology & Hepatology* 2002, **14**:359-363.
29. Wright PA, Williams GT: **Molecular biology and gastric carcinoma.** *Gut* 1993, **34**:145-147.
30. Tahara E: **Genetic Alterations in Human Gastrointestinal Cancers - the Application to Molecular Diagnosis.** *Cancer* 1995, **75**:1410-1417.
31. Lee JS, Grisham JW, Thorgeirsson SS: **Comparative functional genomics for identifying models of human cancer.** *Carcinogenesis* 2005, **26**:1013-1020.
32. Herschkowitz JI, Simin K, Weigman VJ, Mikaelian I, Usary J, Hu ZY, Rasmussen KE, Jones LP, Assefnia S, Chandrasekharan S, Backlund MG, Yin YZ, Khramtsov AI, Bastein R, Quackenbush J, Glazer RI, Brown PH, Green JE, Kopelovich L, Furth PA, Palazzo JP, Olopade OI, Bernard PS, Churchill GA, Van Dyke T, Perou CM: **Identification of conserved gene expression features between murine mammary carcinoma models and human breast tumors.** *Genome Biology* 2007, **8**:R76.
33. He XC, Zhang JW, Tong WG, Tawfik O, Ross J, Scoville DH, Tian Q, Zeng X, He X, Wiedemann LM, Mishina Y, Li LH: **BMP signaling inhibits intestinal stem cell self-renewal through suppression of Wnt-β-catenin signaling.** *Nature Genetics* 2004, **36**:1117-1121.
34. Zhao Y, Geverd DA: **Regulation of Smad3 expression in bleomycin-induced pulmonary fibrosis: a negative feedback loop of TGF-β signaling.** *Biochemical and Biophysical Research Communications* 2002, **294**:319-23.
35. **Gene Expression Omnibus** [http://www.ncbi.nlm.nih.gov/geo/]
36. Sorlie T, Perou CM, Tibshirani R, Aas T, Geisler S, Johnsen H, Hastie T, Eisen MB, Rijn M van de, Jeffrey SS, Thorsen T, Quist H, Matese JC, Brown PO, Botstein D, Lonning PE, Borresen-Dale AL: **Gene expression patterns of breast carcinomas distinguish tumor subclasses with clinical implications.** *Proceedings of the National Academy of Sciences of the United States of America* 2001, **98**:10869-10874.
37. **Stanfrod Microarray Database** [http://genome-www5.stanford.edu/]
38. Kaiser S, Park YK, Franklin JL, Halberg RB, Yu M, Jessen WJ, Freudenberg J, Chen XD, Haigis K, Jegga AG, Kong S, Sakthivel B, Xu H, Reichling T, Azhar M, Boivin GP, Roberts RB, Bissahoyo AC, Gonzales F, Bloom GC, Eschrich S, Carter SL, Aronow JE, Kleimeyer J, Kleimeyer M, Ramaswamy V, Settle SH, Boone B, Levy S, Graff JM, Doetschman T, Groden J, Dove WF, Threadgill DW, Yeatman TJ, Coffey RJ, Aronow BJ: **Transcriptional recapitulation and subversion of embryonic colon development by mouse colon tumor models and human colon cancer.** *Genome Biology* 2007, **8**:R131.
39. Beer DG, Kardia SLR, Huang CC, Giordano TJ, Levin AM, Misek DE, Lin L, Chen GA, Gharib TG, Thomas DG, Lizyness ML, Kuick R, Hayasaka S, Taylor JMG, Iannettoni MD, Orringer MB, Hanash S: **Gene-expression profiles predict survival of patients with lung adenocarcinoma.** *Nature Medicine* 2002, **8**:816-824.
40. **The United States National Cancer Institute website** [https://array.nci.nih.gov/caarray/project/beer-00153]
41. Benjamini Y, Hochberg Y: **Controlling the false discovery rate: A practical and powerful approach to multiple testing.** *Journal of the Royal Statistical Society* 1995, **57**:289-300.
42. Schadt EE, Molony C, Chudin E, Hao K, Yang X, Lum PY, Kasarskis A, Zhang B, Wang S, Suver C, Zhu J, Millstein J, Sieberts S, Lamb J, GuhaThakurta D, Derry J, Storey JD, Avila-Campillo I, Kruger MJ, Johnson JM, Rohl CA, van Nas A, Mehrabian M, Drake TA, Lusis AJ, Smith RC, Guengerich FP, Strom SC, Schuetz E, Rushmore TH, Ulrich R: **Mapping the genetic architecture of gene expression in human liver.** *PLoS Biology* 2008, **6**:e107.

Dietary Tricin Suppresses Inflammation-Related Colon Carcinogenesis in Male Crj: CD-1 Mice

Takeru Oyama,[1] Yumiko Yasui,[1] Shigeyuki Sugie,[1] Mamoru Koketsu,[2] Kunitomo Watanabe[3] and Takuji Tanaka[1,4]

Abstract The flavone 4′,5,7-trihydroxy-3′,5′-dimethoxyflavone (tricin) present in rice, oats, barley, and wheat exhibits antigrowth activity in several human cancer cell lines and anti-inflammatory potential. However, the chemopreventive activity has not yet been elucidated in preclinical animal models of colorectal cancer. This study was designed to determine whether dietary tricin exerts inflammation-associated colon carcinogenesis induced by azoxymethane and dextran sulfate sodium in mice. Male Crj: CD-1 mice were initiated with a single i.p. injection of azoxymethane (10 mg/kg body weight) and followed by a 1-week exposure to dextran sulfate sodium (1.5%, *w/v*) in drinking water to induce colonic neoplasms. They were then given the experimental diet containing 50 or 250 ppm tricin. The experiment was terminated at week 18 to determine the chemopreventive efficacy of tricin. In addition, the effects of dietary tricin on the expression of several inflammatory cytokines, including tumor necrosis factor (TNF)-α, were assayed. The development of colonic adenomas and adenocarcinomas was significantly reduced by feeding with 50 and 250 ppm tricin, respectively. Dietary tricin also significantly reduced the proliferation of adenocarcinoma cells as well as the numbers of mitoses/anaphase bridging in adenocarcinoma cells. The dietary administration with tricin significantly inhibited the expression of TNF-α in the nonlesional cypts. Our findings that dietary tricin inhibits inflammation-related mouse colon carcinogenesis by suppressing the expression of TNF-α in the nonlesional cyrpts and the proliferation of adenocarcinomas suggest a potential use of tricin for clinical trials of colorectal cancer chemoprevention.

Cancer mortality rates in the developed countries have increased throughout this century, and has been already the leading cause of death in some Western countries (1, 2). Great advances have been made in the pharmacologic-based treatment of malignant epithelial malignancies. There has also been a marked increase in the understanding of cell and molecular mechanisms underlying a variety of carcinogenic processes (3). However, therapeutic options for advanced neoplastic disease remain limited. This lack of treatment alternatives may be due to the large number of genetic and molecular alterations associated with advanced neoplasms that contribute to the maintenance of neoplastic progression.

The chemopreventive approach to inhibit cancer development and progression is highly attractive. Practical limitations may exist with respect to developing novel and effective chemopreventive agents through the use of appropriate animal models for preclinical evaluation of candidate chemopreventive agents (4). Some herbal and botanical products that contain flavonoids are likely to possess cancer preventive activities (5). A diet rich in fruits and vegetables has long been suggested to correlate with a reduced risk of certain epithelial malignancies, including cancers in the colon, lung, prostate, oral cavity, and breast (5–7). A number of agents have been reported to be candidate *chemo-inhibitors* of cancer development in various tissues, including colon. Among these agents are the flavonoids, a group of phenolic compounds with structural formula of diphenyl-propane and secondary metabolites produced by plants (5, 8, 9).

4′,5,7-Trihydroxy-3′,5′-dimethoxyflavone (tricin; Fig. 1A) is a flavone, a subgroup of the flavonoid group, which is found *in* rice, oats, barley, and wheat (10). Although the physiologic function of tricin in plants is not well defined, the compound is thought to be produced by the plant during times of environmental stress or pathogenic attack (11) and exert potential allelopathic effects (12). Evidence for the biological activity of tricin in rodents has recently been reported. These biological activities

Authors' Affiliations: [1]Department of Oncologic Pathology, Kanazawa Medical University, Ishikawa, Japan; [2]Divisions of Instrumental Analysis and [3]Anaerobe Research, Life Science Research Center, Gifu University; and [4]The Tohkai Cytopathology Institute: Cancer Research and Prevention, Gifu, Japan
Received 4/3/09; revised 7/7/09; accepted 7/22/09; published OnlineFirst 11/24/09.

Grant support: Grant-in-Aid for Cancer Research, for the Third-Term Comprehensive 10-Year Strategy for Cancer Control from the Ministry of Health, Labour and Welfare of Japan; Grants-in-Aid grant nos. 18592076 (T. Tanaka), 17015016 (T. Tanaka), and 18880030 (Y. Yasui) for Scientific Research from the Ministry of Education, Culture, Sports, Science and Technology of Japan; and grant H2008-12 (T. Tanaka) for the Project Research from the High-Technology Center of Kanazawa Medical University.

Note: Supplementary data for this article are available at Cancer Prevention Research Online (http://cancerprevres.aacrjournals.org/).

Requests for reprints: Takuji Tanaka, Department of Oncologic Pathology, Kanazawa Medical University, 1-1 Daigaku, Uchinada, Ishikawa 920-0293, Japan. Phone: 81-76-218-8116; Fax: 81-76-288-6926; E-mail: takutt@kanazawa-med.ac.jp.

doi:10.1158/1940-6207.CAPR-09-0061

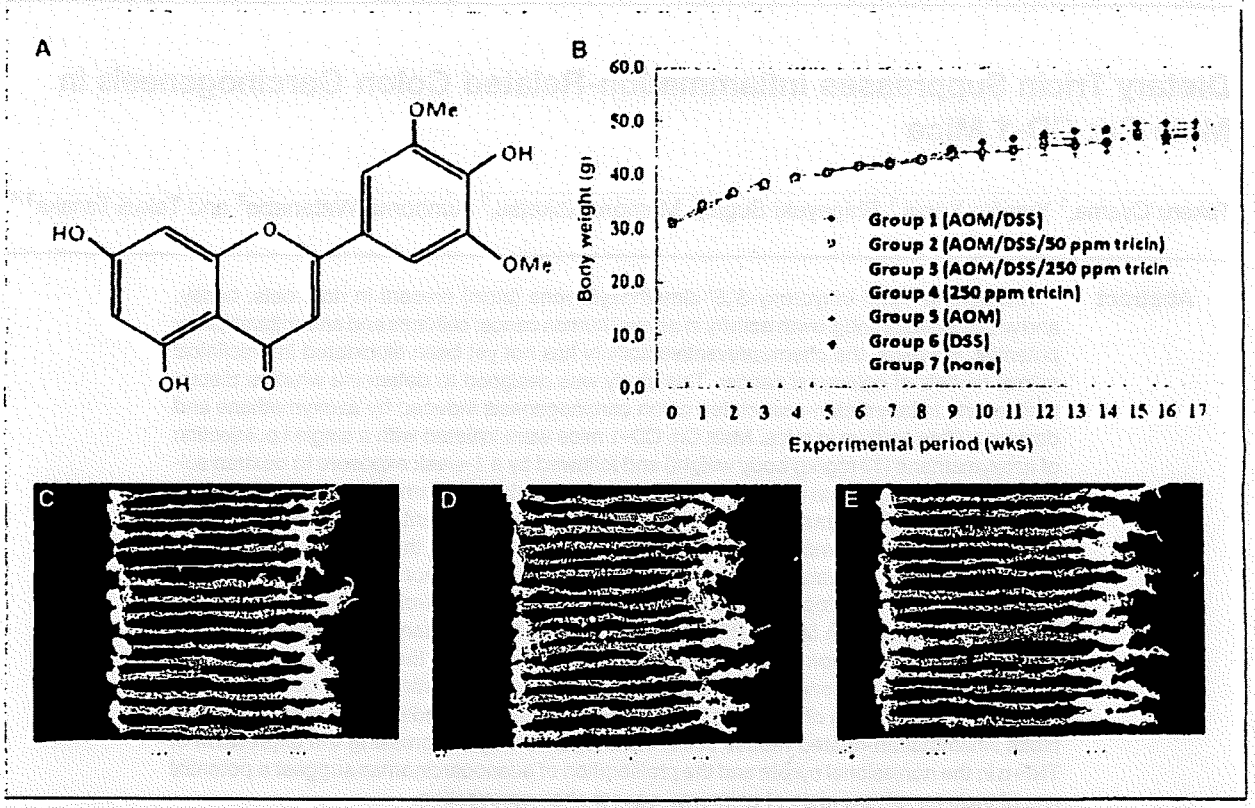

Fig. 1. *A*, the structure of tricin; molecular weight, 330.074. *B*, body weight changes of mice in all groups during the study. Dietary tricin (groups 2, 3, and 5) did not significantly affect the body weight gain. Macroscopic views of the colons from the mice of groups 1 (*C*), 2 (*D*), and 3 (*E*), which received AOM/DSS, AOM/DSS/50 ppm tricin, and AOM/DSS/250 ppm tricin, respectively, at the end of the study (week 18). Although a number of colonic tumors were observed in the mice of group 1, the numbers of the tumors found in groups 2 and 3 were smaller than that in group 1.

include antioxidative (13, 14), antiinflammatory, antiviral (15), and antihistamic (16) activities. These same biological activities have been observed in other promising cancer chemopreventive agents (17–20). The effects of tricin on oncogenesis have been investigated by Gescher et al. Their studies have shown that tricin suppresses the growth of human malignant breast tumor in nude mice (21). Dr. Gescher's group also reported that treatment with tricin-containing extracts from brown rice inhibit the proliferation of human colon and breast cancer cells *in vitro* (22). There are few reports on the effects of dietary tricin on intestinal carcinogenesis. Cai et al. (23) reported that feeding a diet containing 0.2% tricin decreased the size and the number of intestinal adenoma formed in $Apc^{Min/+}$ mice through the inhibition of cyclooxygenase (COX)-2 (23, 24). Dietary tricin did not affect tumor formation in the large bowel (23). Because the concentration of tricin in the mouse intestine is greater than the concentration in the plasma or liver when mice are fed diets containing tricin (25–28), we hypothesized that dietary tricin may affect and possibly inhibit chemically-induced colon carcinogenesis in rodents.

The current study was designed to explore the possible cancer chemopreventive efficacy of tricin. We investigated the effects of dietary tricin on large bowel oncogenesis using an azoxymethane (AOM)/dextran sodium sulfate (DSS)–treated mouse model, which is a useful animal model to study chemoprevention in inflammation-related colon carcinogenesis (29–34). The effects of dietary tricin on the expression of inflammatory enzymes, such as COX-2 (35–37) and inducible nitric oxide synthase (iNOS; refs. 37, 38), and inflammatory cytokines, such as tumor necrosis factor (TNF)-α, (39, 40) NF-κB (17, 40), inhibitor κB (IκB)α, and IκB kinase (IKK)β in the nonlesional colonic mucosa were examined to understand the mechanism(s) by which the compound modify AOM/DSS-induced colon carcinogenesis. In addition, we determined whether dietary tricin affects the chromosomal instability (41) of adenocarcinoma cells by counting the number of anaphase-bridging formations.

Materials and Methods

Chemicals

Tricin (>99% pure confirmed by high performance liquid chromatography) was isolated and prepared from the leaves of *Sasa albo-marginata* (Hououdou Co. Ltd.) by one (M.K.) of the authors (15). In brief, the dried leaves (50 kg) were combined with water (1,000 l) and extracted at 170°C over a period of 3 h. The extracted solution was filtered. The hot water extract of *Sasa albo-marginata* was fractionated successively with ethyl acetate and *n*-butanol. The ethyl acetate fraction (52.0 g) was fractionated using a silica gel 60 (Cica-reagent, 40-50 μm) column (inner diameter 6 × 50 cm, 500 g) and washed with *n*-hexane-ethyl acetate and methanol. This process yielded seven fractions (A-G). Chloroform was added to fraction F (1.50 g) to obtain a chloroform-soluble fraction and an insoluble fraction (solid phase). Tricin (10.0 mg) was recrystallized from the chloroform-soluble fraction as yellow,

needle-shaped crystals. Finally, a total of 8 g of tricin was prepared from 40,000 kg of the leaves and was used in this study.

AOM was purchased from Sigma-Aldrich. DSS with a molecular weight of 36,000 to 50,000 was obtained from MP Biomedicals, LLC. DSS 1.5% (*w/v*) was prepared shortly before use to induce colitis.

Animals and diets

Five-week-old male Crj: CD-1 (ICR) mice were purchased from Charles River Laboratories, Inc. All animals were housed in plastic cages (three or four mice/cage) and had free access to tap water and a basal diet, Charles River Formula-1 (Oriental Yeast, Co., Ltd.). The animals were kept in an experimental animal room under controlled conditions of humidity (50 ± 10%), light (12/12-h light/dark cycle) and temperature (23 ± 2°C). After 1 wk of quarantine, animals were divided into six experimental groups and one control group. Experimental diets were prepared by mixing tricin in powdered basal diet at two dose levels, 50 and 250 ppm. The highest dose was one eighth of the dose used by Cai et al. (23) because we investigated the potential clinical application of low doses of tricin.

Animal experiment

The experimental and study design were approved by the Committee of Kanazawa Medical University Animal Facility under the Institutional Animal Care guideline. All handling and procedures were carried out in accordance with the appropriate Institutional Animal Care Guidelines.

A total of 95 male ICR mice were divided into six experimental groups and one control group. Mice in groups 1 ($n = 20$), 2 ($n = 20$), and 3 ($n = 19$) were given a single i.p. injection of AOM (10 mg/kg body weight). Beginning 7 d after the AOM injection, they also received 1.5% (*w/v*) DSS in drinking water for 7 d. Beginning 1 wk following the final DSS exposure, the mice in groups 2 were fed an experimental diet containing tricin at the rate of 50 ppm and the mice in group 3 were fed an experimental diet containing 250 ppm tricin. Both groups received the experimental diets for 15 wk. The mice in groups 4 ($n = 9$) received only the 250 ppm tricin-containing diet. The mice in group 5 ($n = 9$) received only AOM, and the mice in group 6 ($n = 9$) received only 1.5% DSS in drinking water. The mice of group 7 ($n = 9$) served as untreated controls.

At week 8, four mice each from groups 1, 2, and 3 and three mice each from groups 4, 5, 6, and 7 were randomly selected and sacrificed to measure mRNA expression of target inflammatory enzymes and cytokines in the colonic mucosa by quantitative reverse transcription-PCR (RT-PCR). At sacrifice, the large bowel of each animal was removed, the contents (feces) were washed out by physiologic saline, and the length from the ileocecal junction to the anal verge were measured. After the large bowels were cut open longitudinally along the main axis and gently washed with saline, scraped colonic mucosa tissue was dipped into the RNAlater solution (Applied Biosystems/Ambion).

At week 18, all of the remaining animals were euthanized by exsanguinations through the abdominal aorta under diethylether anesthesia and subjected to a complete gross necropsy examination to determine the incidence and multiplicity of tumors in the large bowel. At sacrifice, the large bowel was removed and the length was measured. Each large bowel was cut open longitudinally along the main axis and gently washed with saline, then examined manually to determine the incidence and multiplicity of tumors. The colon was fixed in 10% buffered formalin for at least 24 h. Histopathologic examination was done on H&E-stained sections made from paraffin-embedded blocks. Colonic tumors were diagnosed according to criteria established in a prior study (34). The number and density of mucosal ulcers on H&E-stained sections was also recorded.

Immunohistochemistry of proliferating cell nuclear antigen

Immunohistochemical analysis for the proliferating cell nuclear antigen (PCNA) in the colon with or without tumors was done on 4-μm-thick paraffin-embedded sections by the labeled avidin-biotin-peroxidase complex method using a Vectastain ABC kit (Vector Laboratories), with microwave accentuation. The paraffin-embedded sections were heated for 30 min at 65°C, deparaffinized in xylene, and rehydrated with ethanol at room temperature. PBS (pH 7.4; 0.01 mol/L) as used to prepare the solutions and for washes between the preparation steps. Incubations were done in a humidified chamber. The sections were treated for 40 min at room temperature with mouse IgG blocking reagent (Vector Laboratories), and incubated overnight at 4°C with the primary antibody (1:300 dilution; DAKO Japan, Co., Ltd.). The antibody was applied to the sections according to the manufacturer's protocol. Horseradish peroxidase activity was visualized by treatment with H_2O_2 (DAKO Japan, Co., Ltd.) and 3,3'-diaminobenzidine (DAKO Japan) for 5 min. In the last step, the sections were weakly counterstained with Mayer's hematoxylin (Merck). For each examination, negative controls were done on serial sections. The numbers of nuclei with positive reactivity for PCNA-immunohistochemistry were counted by two observers (T.O. and T.T.) who were unaware of the treatment groups to which the slides belonged. The positive rates were evaluated in >100 cancer cells each of 15 different areas of the adenocarcinomas and 10 different crypts of the "normal"-appearing colonic mucosa from five mice each from groups 1 to 3 and expressed as percentage (mean ± SD).

Mitotic index and anaphase bridging index of adenocarcinoma cells

To examine the effects of dietary tricin on chromosomal instability (41) in adenocarcinoma cells, the anaphase bridging index (ABI) was determined on H&E-stained sections. The numbers of mitoses and anaphase bridging were counted in >100 cancer cells from five adenocarcinomas each from groups 1 through 3. The mitotic index (MI; number of mitoses per cancer cells) and ABI (number of anaphases with bridging per mitoses) were expressed as percentages (mean ± SD).

Quantitative RT-PCR

The normal-appearing colonic mucosa of mice from groups 1 through 3 were assayed for mRNA expression of COX-2, iNOS, TNF-α, NF-κB, IκBα, and IKKβ by RT-PCR. RNA was extracted using the RNeasy Mini kit (Qiagen) according to the manufacturer's protocol. cDNA was synthesized from 0.2 μg of total RNA using SuperScript III First-Strand Synthesis System (Invitrogen Co.). Real-time PCR was done in a LightCycler (Roche Diagnostics Co.) with SYBR Premix Ex Taq (TAKARA BIO, INC.). The expression level of each gene was normalized to the β-actin expression level using the standard curve method. Each assay was done six times and the average was calculated. The primers used for amplifications are listed in Supplementary Table S1.

Statistical analysis

Where applicable, data were analyzed using one-way ANOVA with Tukey-Kramer Multiple Comparisons Test or Bonferroni (GraphPad Instat version 3.05, GraphPad Software) with $P < 0.05$ as the limit for statistical significance. Fisher's Exact Probability test or the χ^2 test were used for comparison of the incidence of lesions between the two groups. Data on mRNA expression (mean ± SEM) were analyzed by Mann-Whitney *U* test.

Results

General observation

All animals remained healthy throughout the experimental period. Food consumption (grams/day/mouse) did not differ significantly among the groups (data not shown). The body weight gains by mice in all of the seven groups were similar during the study (Fig. 1B). The mean body weight of group 2 (AOM/DSS/50 ppm tricin) was significantly lower than that of group 1 ($P < 0.01$; Supplementary Table S2). The mean colon length of group 1 was significantly shorter than the mean

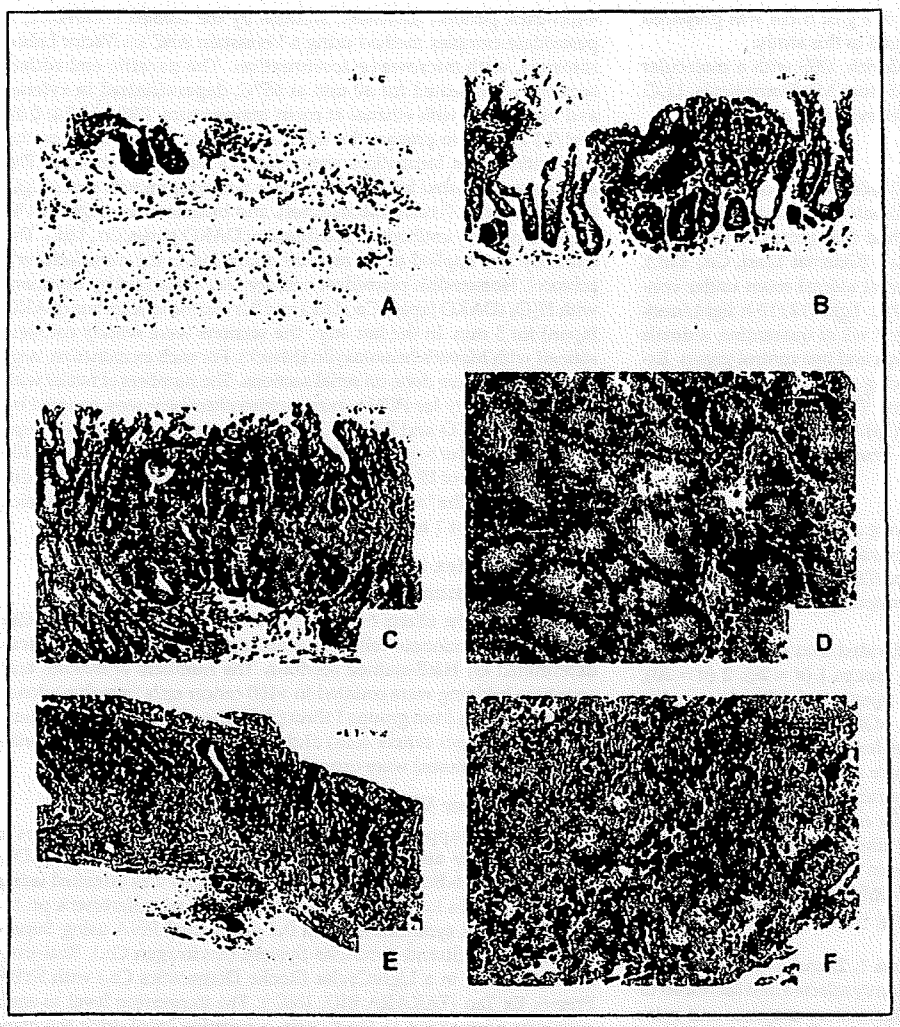

Fig. 2. Representative histopathology of the colonic lesions in group 1 (AOM/DSS). *A*, mucosal ulcer; *B*, dysplastic crypts; *C* and *D*, tubular adenomas; *E* and *F*, moderately differentiated tubular adenocarcinomas.

colon length of group 7 (no treatment; $P < 0.01$; Supplementary Table S2).

Incidence and multiplicity of colonic lesions

The incidence of macroscopic colonic lesions, including tumors and small ulcerations, were seen in the mice in group 1, 2, 3, and 6 (Fig. 1C-E). All mice in groups 1 through 3, which were treated with AOM/DSS with or without tricin, developed colonic tumors (adenoma and/or adenocarcinoma). The mice of group 4, 5, and 7 did not develop colonic tumors.

Microscopic examinations revealed various pathologic colonic lesions in mice from groups 1, 2, 3, and 6. The lesions included mucosal ulcers (Fig. 2A), dysplastic crypts (Fig. 2B), tubular adenomas (Fig. 2C and D), and tubular adenocarcinomas (Fig. 2E and F). Some of the adenocarcinomas that developed in the group 1 mice invaded the subserosa of the colon (Fig. 2E). Table 1 summarizes the microscopic data on the incidence and multiplicity of colonic lesions. The dietary administration of 50 ppm tricin (group 2) significantly reduced the incidence ($P = 0.0117$) and multiplicity ($P < 0.05$) of adenomas and the number of total tumors (adenoma + adenocarcinoma, $P < 0.05$) when compared with group 1. Feeding with 250 ppm tricin (group 3) also significantly lowered the numbers of adenocarcinomas and total tumors when compared with group 1 ($P < 0.05$ for each comparison). The mean numbers of dysplastic crypts in groups 2 ($P < 0.05$) and 3 ($P < 0.01$) were significantly lower than that of dysplastic crypts in group 1. The mean numbers of mucosal ulcers in group 2 ($P < 0.05$) and 3 ($P < 0.001$) were also significantly smaller than that of group 1.

PCNA labeling indices of the normal-appearing crypts and adenocarcinomas

The data on the proliferative kinetics in the normal-appearing crypts and colonic adenocarcinomas by estimating the PCNA labeling indices are shown in Fig. 3. The dietary administration of tricin significantly lowered the PCNA labeling index of the normal-appearing crypts in group 2 (38 ± 11, $P < 0.05$) and group 3 (36 ± 12, $P < 0.05$) when compared with group 1 (48 ± 11). The PCNA labeling indices for colonic adenocarcinomas in groups 2 (74 ± 6, $P < 0.05$) and 3 (71 ± 4, $P < 0.001$) were significantly lower than in group 1 (80 ± 8).

Table 1. Incidence and multiplicity of colonic lesions

Group no.	Treatment (no. of mice examined)	Mucosal ulcer	Dysplasia (high grade)	Adenoma	Adenocarcinoma	Total tumors (AD+ADC)
1	AOM/1.5% DSS (16)	100% (2.69 ± 0.95)*	100% (5.00 ± 3.79)	88% (4.19 ± 4.22)	94% (4.63 ± 3.74)	94% (8.81 ± 6.21)
2	AOM/1.5% DSS/50 ppm tricin (16)	94% (1.81 ± 1.11)	80% (2.56 ± 1.79)†,‡	44%§ (1.44 ± 1.79)†,‡	75% (3.19 ± 2.64)	75% (4.63 ± 4.05)†,‡
3	AOM/1.5% DSS/250 ppm tricin (15)	60% (0.87 ± 0.83)∥	73% (1.53 ± 1.13)¶	67% (1.87 ± 1.73)	67% (1.80 ± 2.04)†,‡	80% (3.67 ±3.37)†,‡
4	250 ppm tricin (6)	0%	0%	0%	0%	0%
5	AOM (6)	0%	0%	0%	0%	0%
6	1.5% DSS (6)	33% (0.33 ± 0.52)	0%	0%	0%	0%
7	None (6)	0%	0%	0%	0%	0%

Abbreviations: AD, adenoma; ADC, adenocarcinoma.
*Mean ± SD.
†Significantly different from group 1 by one-way ANOVA, and Tukey-Kramer Multiple Comparisons test.
‡$P < 0.05$.
§Significantly different from group 1 by Fisher's exact probability test ($P = 0.0117$).
∥$P < 0.001$.
¶$P < 0.01$.

The effects of tricin on the MI and ABI

Dietary administration with tricin affected the number of mitosis (Fig. 4A) and anaphase bridging (Fig. 4B) in adenocarcinomas. As illustrated in Fig. 4C, dietary feeding with tricin significantly decreased the MI in group 2 (17.4 ± 0.9, $P < 0.05$) and group 3 (12.7 ± 2.0, $P < 0.001$) compared with group 1 (20.8 ± 2.4). The treatment also lowered the ABI in group 2 (0.50 ± 0.24) and group 3 (0.29 ± 0.10, $P < 0.05$) compared with group 1 (1.10 ± 0.57).

Expressions of inflammatory enzyme and cytokine genes in colonic mucosa

At week 8, we assayed mRNA levels of COX-2, iNOS, TNF-α, NF-κB, IκBα, and IKKβ in the nonlesional colonic mucosa of

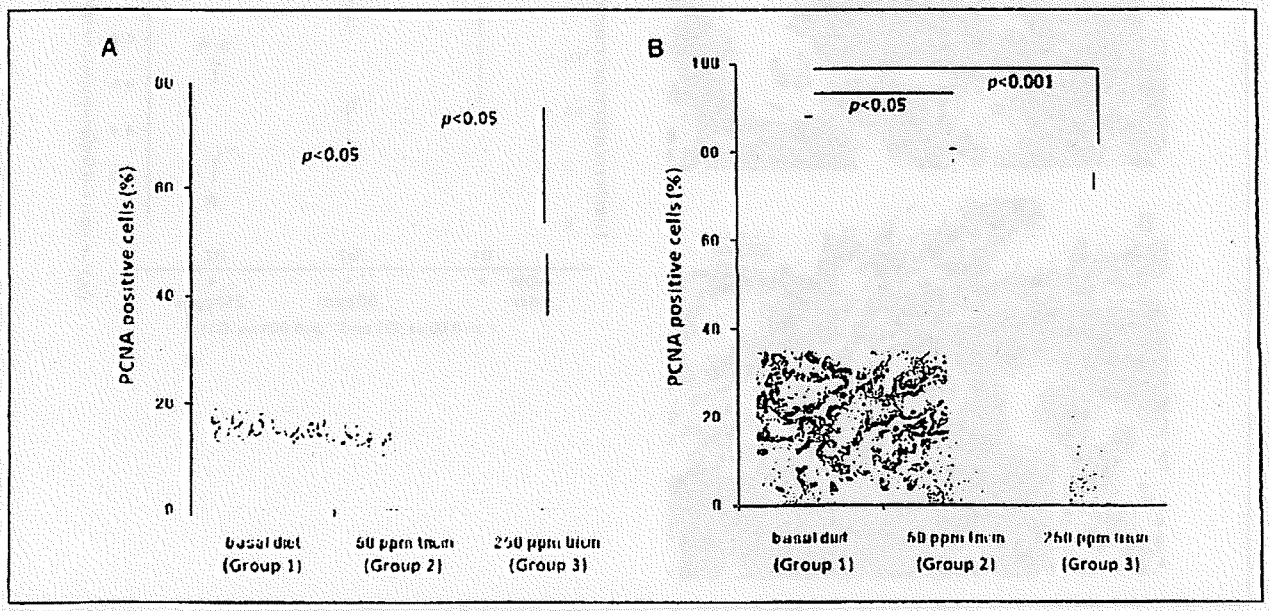

Fig. 3. The PCNA labeling indices of the normal-appearing crypts (*A*) and adenocarcinomas (*B*). Feeding with tricin (groups 2 and 3) significantly lowered the PCNA labeling indices of the normal-appearing crypts ($P < 0.05$ for each comparison) and adenocarcinomas (group 2, $P < 0.05$; and group 3, $P < 0.001$) compared with group 1.

mice in groups 1 through 3 by semiquantitative real-time RT-PCR (Fig. 5). The TNF-α expression significantly decreased in group 3 compared with group 1 ($P < 0.05$; Fig. 5A). Feeding with tricin did not significantly affect the expression of COX-2 (Fig. 5B), iNOS (Fig. 5C), NF-κB (Fig. 5D), IκBα (Fig. 5E), and IKKβ (Fig. 5F).

Discussion

The results described herein clearly indicate that dietary administration with tricin at two dose levels (50 and 250 ppm) significantly inhibited AOM/DSS-induced colonic tumorigenesis in male ICR mice. The high dose (250 ppm) of tricin significantly inhibited development of adenocarcinomas induced by AOM followed by DSS in mice. The dietary administration with tricin also significantly affected the expression of TNF-α in the colonic mucosa at week 8. The treatment resulted in the reduction of the PCNA labeling index, MI, and ABI in the colonic epithelial malignancies at week 18.

The antitumor and chemoprevention activities of tricin have been reported in both *in vitro* and *in vivo* studies. *In vivo* experiments included transplanted human breast cancer cell lines in nude mice (21). In addition, Cai et al. reported that 0.2% tricin in diet effectively inhibited the number of adenomas in the small intestine of $Apc^{Min/+}$ mice (42). They did not, however, observe inhibition of the development of colonic tumors (42). In the current study, we observed the cancer chemopreventive activity of dietary tricin in carcinogenesis in the inflamed colon. In addition, feeding with tricin lowered the occurrence of mucosal ulcers and preneoplasms (dysplastic crypts).

We can point several mechanisms by which tricin may suppress AOM/DSS-induced colon carcinogenesis in this study. Our findings that dietary tricin lowered the PCNA labeling index, MI, and ABI of colonic adenocarcinomas may suggest an antigrowth effect of tricin on colonic malignancy. The findings are in agreement with the reports by Cai et al. (21) that showed tricin or tricin-containing extracts of brown rice inhibited the growth of the colon and mammary cells *in vitro* and *in vivo* (22). In addition, the results that dietary tricin lowered the ABI of adenocarcinoma cells suggest that tricin affects the chromosomal instability of cancer cells and possibly their telomerase activity (41). Tricin may exert chemopreventive activity through inhibition of COX-1 and 2 enzymes and prostaglandin E_2 production in human colon cancer cell lines (HT-29 and HCA-7) and the small intestine of $Apc^{Min/+}$ mice (23, 24). Unexpectedly, dietary tricin did not significantly alter the expression of COX-2 or iNOS at week 8. The suppression of NF-κB–signaling pathway by dietary administration with tricin was insignificant. However,

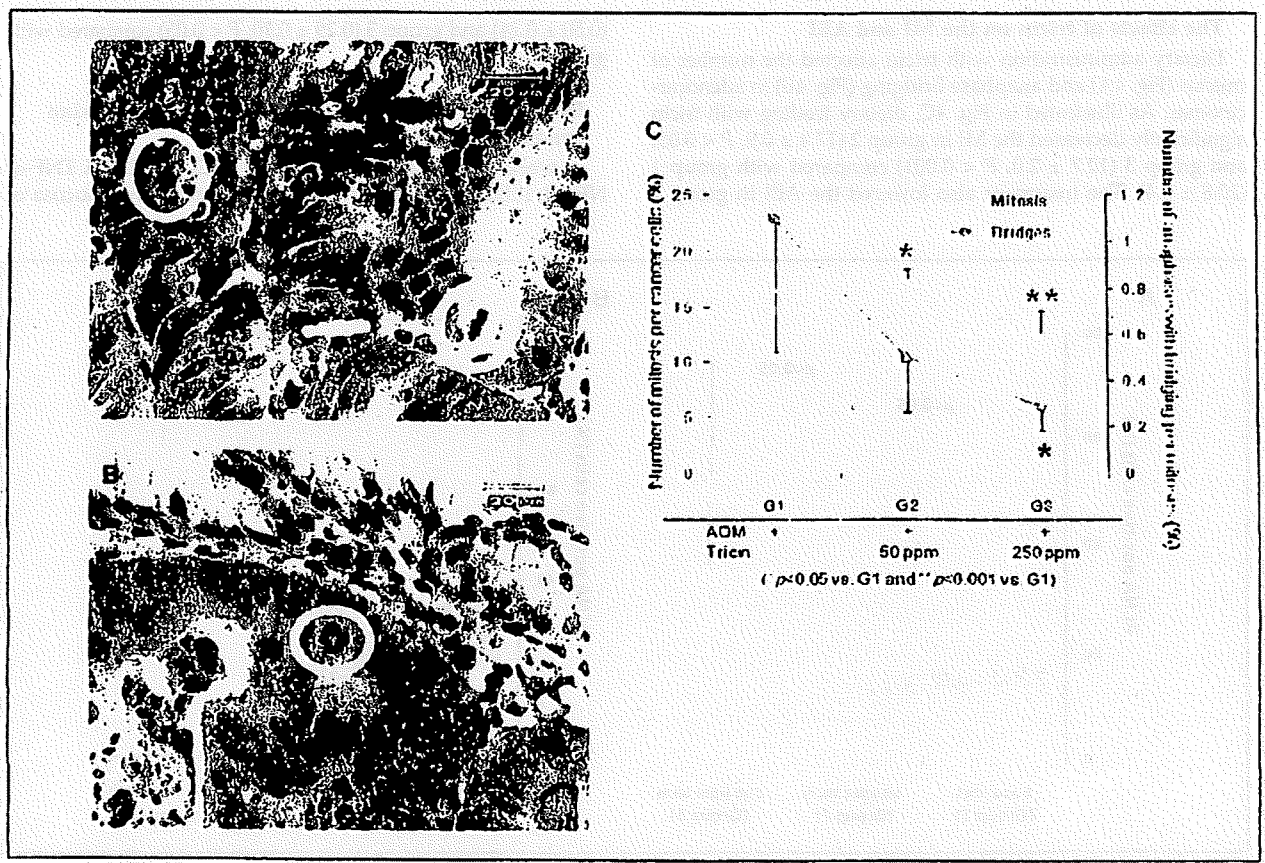

Fig. 4. The effects of dietary tricin on the MI and ABI. *A*, representative mitotic figures (*left circle*, anaphase; *right circle*, metaphase) in an adenocarcinoma, (*B*) representative anaphase bridging (*circle*) in an adenocarcinoma, and (*C*) MI (*columns*) and ABI (*lines*). Dietary administration of tricin significantly reduced the MI (50 ppm tricin, $P < 0.05$; and 250 ppm tricin, $P < 0.001$) and ABI (250 ppm tricin, $P < 0.05$). *G1*, group1; *G2*, group2; and *G3*, group 3.

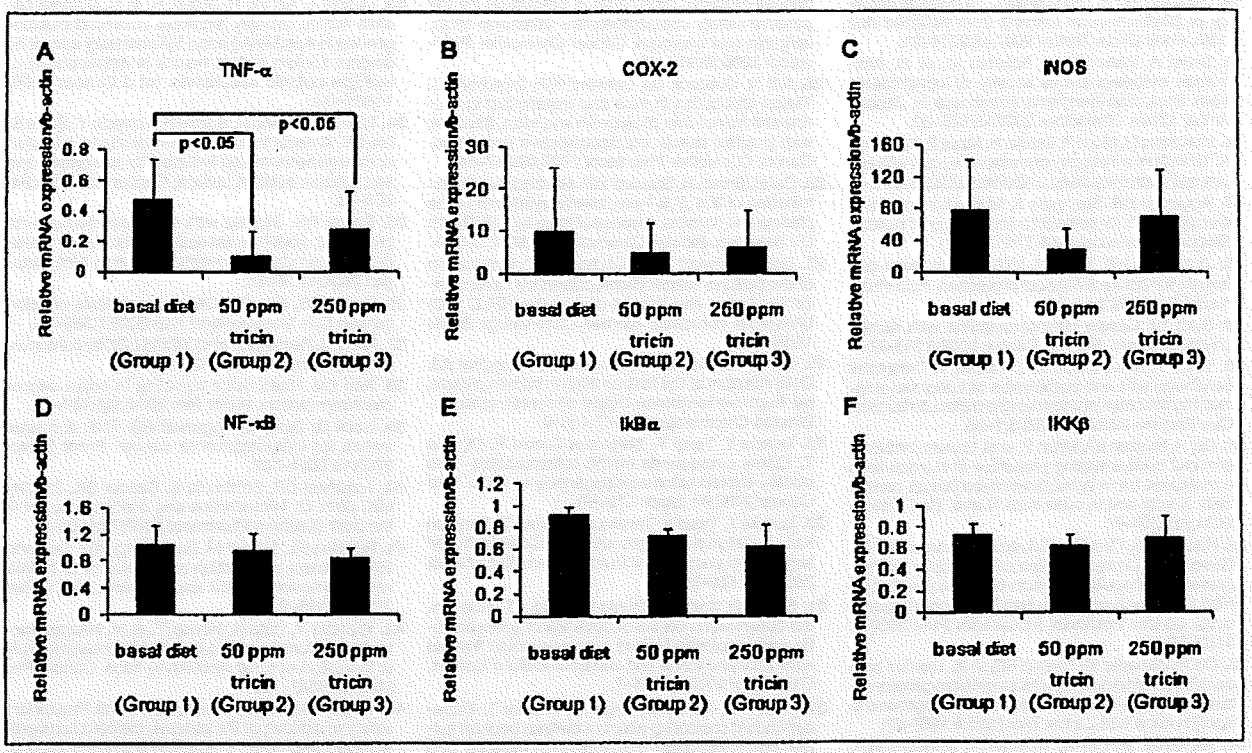

Fig. 6. The expression of (A) TNF-α (B) COX-2, (C) INOS, (D) NF-κB, (E) IκBα, and (F) IKKβ in the normal-appearing colonic mucosa of groups 1 to 3 that were assessed by semiquantitative real-time RT-PCR. The expression of TNF-α was significantly inhibited by feeding with tricin (groups 2 and 3, $P < 0.05$ for each comparison). Feeding with tricin lowered the expression of COX-2, iNOS, and the NF-κB signaling pathway, but the reduction did not reach statistical significance. The expression was normalized to β-actin mRNA expression. Samples were analyzed in triplicate. *Columns*, mean of three independent experiments; *bars*, SEM; $n = 12$, Statistical analysis was done by the Mann-Whitney *U* test.

we observed that dietary tricin significantly inhibited the expression of TNF-α in the nonlesions colonic mucosa. Such effects are of interest because TNF-α acts as a master switch to establish an intricate link between inflammation and cancer (39, 40).

In conclusion, the dietary administration with tricin effectively suppressed AOM/DSS-induced colon carcinogenesis by suppressing the expression of TNF-α in the early phase and MI and ABI in the later phase. The effects of tricin on TNF-α expression are also important in the chemopreventive activity of tricin in inflammation-associated colorectal carcinogenesis. The safety of tricin was reported by Verschoyle et al. (43). A natural flavonoid tricin is present in edible plants, including rice, oats, barley, and wheat (10). In the current study, we isolated tricin from the dried leaves of *Sasa albo-marginata* that contain a large amount (0.2 ppm) of tricin than rice (Oryza sativa L.; 0.066 ppm). Tricin is thus a candidate for clinical use for fighting colorectal cancer development in patients without colitis.

Disclosure of Potential Conflicts of Interest

No potential conflicts of interest were disclosed.

References

1. Jemal A, Siegel R, Ward E, et al. Cancer statistics, 2008. CA Cancer J Clin 2008;58:71–96.
2. Karim-Kos HE, de Vries E, Soerjomataram I, Lemmens V, Siesling S, Coebergh JW. Recent trends of cancer in Europe: a combined approach of incidence, survival and mortality for 17 cancer sites since the 1990s. Eur J Cancer 2008;44:1345–89.
3. Tanaka T. Colorectal carcinogenesis: review of human and experimental animal studies. J Carcinog 2009;8:5.
4. Rosenberg DW, Giardina C, Tanaka T. Mouse models for the study of colon carcinogenesis. Carcinogenesis 2009;30:183–96.
5. Tanaka T. Effect of diet on human carcinogenesis. Crit Rev Oncol Hematol 1997;25:73–95.
6. Tanaka T, Miyamoto S, Suzuki R, Yasui Y. Chemoprevention of colon carcinogenesis by dietary nonnutritive compounds. Curr Top Neutraceut Res 2006;4:127–52.
7. Tanaka T, Oyama T, Yasui Y. Dietary supplements and colorectal cancer. Curr Topics Neutarceut Res 2008;6:165–88.
8. Murthy NS, Mukherjee S, Ray G, Ray A. Dietary factors and cancer chemoprevention: an overview of obesity-related malignancies. J Postgrad Med 2009;55:45–54.
9. Pan MH, Ho CT. Chemopreventive effects of natural dietary compounds on cancer development. Chem Soc Rev 2008;37:2558–74.
10. Wang HK, Xia Y, Yang ZY, Natschke SL, Lee KH. Recent advances in the discovery and development of flavonoids and their analogues as antitumor and anti-HIV agents. Adv Exp Med Biol 1998;439:191–225.
11. Park HS, Lim JH, Kim HJ, Choi HJ, Lee IS. Antioxidant flavone glycosides from the leaves of Sasa borealis. Arch Pharm Res 2007;30:161–6.
12. Fiorentino A, D'Abrosca B, Pacifico S, et al. Potential allelopatic effects of stilbenoids and flavonoids from leaves of Carex distachya Desf. Biochem Syst Ecol 2008;36:691–8.
13. Duarte-Almeida JM, Negri G, Salatino A, de Carvalho JE, Lajolo FM. Antiproliferative and antioxidant activities of a tricin acylated glycoside from sugarcane (Saccharum officinarum) juice. Phytochemistry 2007;68:1165–71.

14. Renuka Devi R, Arumughan C. Antiradical efficacy of phytochemical extracts from defatted rice bran. Food Chem Toxicol 2007;45:2014–21.
15. Sakai A, Watanabe K, Koketsu M, et al. Anti-human cytomegalovirus activity of constituents from Sasa albo-marginata (Kumazasa in Japan). Antivir Chem Chemother 2008;19:125–32.
16. Kuwabara H, Mouri K, Otsuka H, Kasai R, Yamasaki K. Tricin from a malagasy connaraceous plant with potent antihistaminic activity. J Nat Prod 2003;66:1273–5.
17. Aggarwal BB, Shishodia S. Molecular targets of dietary agents for prevention and therapy of cancer. Biochem Pharmacol 2006;71:1397–421.
18. Janakiram NB, Rao CV. Molecular markers and targets for colorectal cancer prevention. Acta Pharmacol Sin 2008;29:1–20.
19. Surh YJ. Cancer chemoprevention with dietary phytochemicals. Nat Rev Cancer 2003;3:768–80.
20. Yasui Y, Kim M, Oyama T, Tanaka T. Colorectal carcinogenesis and suppression of tumor development by inhibition of enzymes and molecular targets. Curr Enzyme Inhibition 2009;5:1–26.
21. Cai H, Hudson EA, Mann P, et al. Growth-inhibitory and cell cycle-arresting properties of the rice bran constituent tricin in human-derived breast cancer cells *in vitro* and in nude mice *in vivo*. Br J Cancer 2004;91:1364–71.
22. Hudson EA, Dinh PA, Kokubun T, Simmonds MS, Gescher A. Characterization of potentially chemopreventive phenols in extracts of brown rice that inhibit the growth of human breast and colon cancer cells. Cancer Epidemiol Biomarkers Prev 2000;9:1163–70.
23. Cai H, Al-Fayez M, Tunstall RG, et al. The rice bran constituent tricin potently inhibits cyclooxygenase enzymes and interferes with intestinal carcinogenesis in ApcMin mice. Mol Cancer Ther 2005;4:1287–92.
24. Al-Fayez M, Cai H, Tunstall R, Steward WP, Gescher AJ. Differential modulation of cyclooxygenase-mediated prostaglandin production by the putative cancer chemopreventive flavonoids tricin, apigenin and quercetin. Cancer Chemother Pharmacol 2006;58:816–25.
25. Cai H, Boocock DJ, Steward WP, Gescher AJ. Tissue distribution in mice and metabolism in murine and human liver of apigenin and tricin, flavones with putative cancer chemopreventive properties. Cancer Chemother Pharmacol 2007;60:257–66.
26. Cai H, Brown K, Steward WP, Gescher AJ. Determination of 3',4',5',5,7-pentamethoxyflavone in the plasma and intestinal mucosa of mice by HPLC with UV detection. Biomed Chromatogr 2009;23:335–9.
27. Cai H, Steward WP, Gescher AJ. Determination of the putative cancer chemopreventive flavone tricin in plasma and tissues of mice by HPLC with UV-visible detection. Biomed Chromatogr 2005;19:518–22.
28. Cai H, Verschoyle RD, Steward WP, Gescher AJ. Determination of the flavone tricin in human plasma by high-performance liquid chromatography. Biomed Chromatogr 2003;17:435–9.
29. Tanaka T, Yasui Y, Ishigamori-Suzuki R, Oyama T. Citrus compounds inhibit inflammation- and obesity-related colon carcinogenesis in mice. Nutr Cancer 2008;60 Suppl 1:70–80.
30. Tanaka T, Yasui Y, Tanaka M, Oyama T, Rahman KM. Melatonin suppresses AOM/DSS-induced large bowel oncogenesis in rats. Chem Biol Interact 2009;177:128–36.
31. Suzuki R, Kohno H, Sugie S, Tanaka T. Sequential observations on the occurrence of preneoplastic and neoplastic lesions in mouse colon treated with azoxymethane and dextran sodium sulfate. Cancer Sci 2004;95:721–7.
32. Suzuki R, Kohno H, Sugie S, Tanaka T. Dose-dependent promoting effect of dextran sodium sulfate on mouse colon carcinogenesis initiated with azoxymethane. Histol Histopathol 2005;20:483–92.
33. Tanaka T, Kohno H, Suzuki R, et al. Dextran sodium sulfate strongly promotes colorectal carcinogenesis in Apc(Min/+) mice: inflammatory stimuli by dextran sodium sulfate results in development of multiple colonic neoplasms. Int J Cancer 2006;118:25–34.
34. Tanaka T, Kohno H, Suzuki R, Yamada Y, Sugie S, Mori H. A novel inflammation-related mouse colon carcinogenesis model induced by azoxymethane and dextran sodium sulfate. Cancer Sci 2003;94:965–73.
35. Reddy BS. Studies with the azoxymethane-rat preclinical model for assessing colon tumor development and chemoprevention. Environ Mol Mutagen 2004;44:26–35.
36. Reddy BS, Rao CV. Chemoprophylaxis of colon cancer. Curr Gastroenterol Rep 2005;7:389–95.
37. Rao CV. Regulation of COX and LOX by curcumin. Adv Exp Med Biol 2007;595:213–26.
38. Rao CV. Nitric oxide signaling in colon cancer chemoprevention. Mutat Res 2004;555:107–19.
39. Sethi G, Sung B, Aggarwal BB. TNF: a master switch for inflammation to cancer. Front Biosci 2008;13:5094–107.
40. Aggarwal BB, Shishodia S, Sandur SK, Pandey MK, Sethi G. Inflammation and cancer: how hot is the link? Biochem Pharmacol 2006;72:1605–21.
41. Rudolph KL, Millard M, Bosenberg MW, DePinho RA. Telomere dysfunction and evolution of intestinal carcinoma in mice and humans. Nat Genet 2001;28:155–9.
42. Yamada Y, Hata K, Hirose Y, et al. Microadenomatous lesions involving loss of Apc heterozygosity in the colon of adult Apc(Min/+) mice. Cancer Res 2002;62:6387–70.
43. Verschoyle RD, Greaves P, Cai H, et al. Preliminary safety evaluation of the putative cancer chemopreventive agent tricin, a naturally occurring flavone. Cancer Chemother Pharmacol 2006;57:1–6.

Induction of Prostaglandin E_2 Pathway Promotes Gastric Hamartoma Development with Suppression of Bone Morphogenetic Protein Signaling

Hiroko Oshima,[1] Hiraku Itadani,[2] Hidehito Kotani,[2] Makoto Mark Taketo,[3] and Masanobu Oshima[1]

[1]Division of Genetics, Cancer Research Institute, Kanazawa University, Kanazawa, Japan; [2]Oncology Department, Banyu Tsukuba Research Institute, Tsukuba, Japan; and [3]Department of Pharmacology, Kyoto University Graduate School of Medicine, Kyoto, Japan

Abstract

Mutations in bone morphogenetic protein (BMP) receptor 1A (*BMPR1A*) are responsible for a subset of cases of juvenile polyposis (JP) syndrome that develops hamartomatous tumors in the gastrointestinal tract. Mouse genetic studies have shown that suppression of BMP signaling in the intestines causes JP-type hamartoma development. Here, we generated *K19-Nog* transgenic mice expressing noggin, a BMP antagonist, in gastric epithelium. However, inhibition of BMP signaling did not cause gastric phenotypes. We thus crossed *K19-Nog* with *K19-C2mE* mice that expressed *Ptgs2* and *Ptges* in the stomach to generate compound transgenic mice. Expression of *Ptgs2* and *Ptges* results in prostaglandin E_2 (PGE_2) biosynthesis, and both enzymes are induced in most human gastrointestinal tumors. Importantly, *K19-Nog/C2mE* compound mice developed gastric hamartomas that were morphologically similar to those found in JP with mucin-containing dilated cysts and inflammatory infiltration. Notably, treatment of *K19-Nog/C2mE* mice with a cyclooxygenase-2 inhibitor, celecoxib, significantly reduced tumor size with suppression of angiogenesis, suggesting that induction of the PGE_2 pathway together with inhibition of BMP signaling is required for gastric hamartoma development. Moreover, microarray analyses revealed that canonical Wnt signaling target genes were not induced in *K19-Nog/C2mE* hamartomas, indicating that BMP inhibition and PGE_2 induction lead to gastric hamartoma development independent of the Wnt/β-catenin pathway. These results, taken together, suggest that the PGE_2 pathway is an effective preventive target against BMP-suppressed gastric hamartomas, as well as for Wnt/β-catenin–activated adenocarcinomas. [Cancer Res 2009;69(7):2729–33]

Introduction

Juvenile polyposis (JP) is a hereditary gastrointestinal hamartomatous polyposis syndrome (1). Germline mutations in bone morphogenetic protein (BMP) receptor type IA gene (*BMPR1A*) have been found in a subpopulation of JP patients (2). BMP ligands bind to a complex of the BMP receptor type II and type I, which leads to phosphorylation of Smad1,5,8, allowing them to form a complex with Smad4 (3, 4). These Smad complexes translocate to nuclei and function as transcription enhancers. BMP signaling inhibits epithelial cell proliferation and promotes differentiation (5, 6), and suppression of BMP signaling in mice results in intestinal hamartomatous polyp development through activation of the PI3K-Akt pathway (6, 7). Moreover, intestinal epithelial cell–specific deletion of *Bmpr1a* results in elongated villi and crypt fission (8). These results indicate that BMP signaling promotes intestinal epithelial differentiation, and, thus, suppression of the BMP pathway causes tumorigenesis. Although the main affected site of tumors in JP patients is the colon, gastric polyps have been found in 14% of JP patients, and cancer risk in JP patients increases both in the colon and stomach (9, 10). Recently, it was reported that disruption of *Bmpr1a* in mouse stomach results in development of tumorous lesions in squamocolumnar and gastrointestinal transition zones, suggesting that suppression of BMP signaling triggers tumor development also in the stomach (11).

On the other hand, we found that expression of cyclooxigenase-2 (COX-2) and microsomal prostaglandin E synthase-1 (mPGES-1) is induced simultaneously in gastrointestinal tumor tissues (12). COX-2 and mPGES-1 are functionally coupled for biosynthesis of prostaglandin E_2 (PGE_2; ref. 13) that plays a critical role in tumorigenesis in the gastrointestinal tract (14–17). However, the role of the PGE_2 pathway in hamartomatous tumors is not understood. We constructed transgenic mice expressing *Nog* encoding noggin in the gastric mucosa and crossed them with another transgenic mice expressing both *Ptgs2* and *Ptges* encoding COX-2 and mPGES-1, respectively, (16). We show that inhibition of BMP signaling is not sufficient for gastric tumorigenesis, but that BMP suppression together with PGE_2 induction causes development of JP-type gastric hamartoma.

Materials and Methods

Mouse models. *K19-C2mE* mice expressing *Ptgs2* and *Ptges*; *K19-Wnt1* mice expressing *Wnt1*; and *K19-Wnt1/C2mE* mice expressing *Wnt1*, *Ptgs2*, and *Ptges*, were described previously (16, 17). pK19-Nog was constructed using keratin 19 gene promoter, mouse *Nog* cDNA, and SV40 p(A) cassette (Fig. 1*A*). The expression vector was microinjected into the fertilized eggs of F1 (C3H and C57BL/6) mice (CLEA) to generate *K19-Nog* mice. Primer sequences used for genotyping were as follows: F-5′-GTACGCGTGGAATGACCTAGG-3′, F-5′-GCAAAGGGTCGCTACAGACGT-3′. Transgenic vector constructs are shown in Fig. 1*A*. *K19-Nog* and *K19-C2mE* mice were crossed to generate *K19-Nog/C2mE* mice. Gastric phenotypes of these mice were examined at age 30 wk. For inhibition of COX-2, mice were given p.o. with celecoxib (Pfizer) at 100 mg/kg/d for 3 wk. All animal experiments were carried out according to the protocol approved by Ethics Committees on Animal Experimentation of Kanazawa University.

Real-time reverse transcription-PCR. Total RNA was reverse-transcribed and PCR-amplified. Primer sets used in real-time reverse

Note: Supplementary data for this article are available at Cancer Research Online (http://cancerres.aacrjournals.org/).

Requests for reprints: Masanobu Oshima, Division of Genetics, Cancer Research Institute, Kanazawa University, 13-1 Takara-machi, Kanazawa 920-0934, Japan. Phone: 81-76-265-2721; Fax: 81-76-234-4519; E-mail: oshimam@kenroku.kanazawa-u.ac.jp.

doi:10.1158/0008-5472.CAN-08-4394

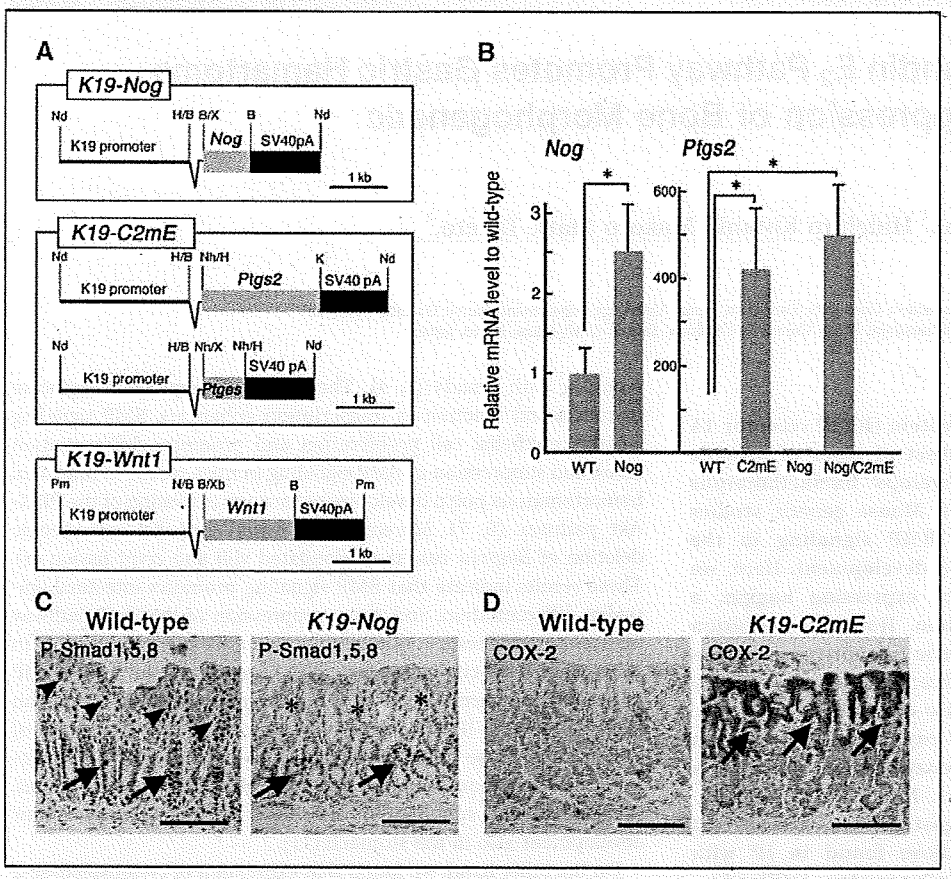

Figure 1. Generation of transgenic mice. *A*, transgenic vectors. *B*, relative mRNA levels (mean ± SD) of *Nog* and *Ptgs2* in the gastric mucosa of *K19-Nog* (*Nog*), *K19-C2mE* (*C2mE*), and *K19-Nog/C2mE* (*Nog/C2mE*) mice to the wild-type (*WT*). *, $P < 0.05$. *C*, immunohistochemistry of phosphorylated Smad1,5,8 in gastric mucosa of wild-type and *K19-Nog* mice. *Arrowheads* and *arrows*, positive nuclear staining in surface and gland bottom, respectively. *Asterisks*, decreased immunostaining signal in *K19-Nog* mouse. *D*, immunohistochemistry of COX-2 in wild-type and *K19-C2mE* mouse stomach. *Arrows*, transgenic expression of COX-2 in *K19-C2mE* gastric mucosa where *K19* promoter is transcriptionally active. *Bars*, 100 μm.

transcription-PCR for detection of *Nog, Ptgs2, Ptger1, Ptger2, Ptger3*, and *Ptger4* were purchased (TakaraBio).

Histology. Tissues were fixed in 4% paraformaldehyde, paraffin embedded, and sectioned at 4-μm thickness. The following antibodies were used for immunostaining: anti–COX-2 (Cayman Chemical), anti-F4/80 (Serotec), anti-α-smooth muscle actin (Sigma), anti–Ki-67, anti-von Willebrand factor (DakoCytomation), and anti–phosphorylated Smad1,5,8 (Chemicon). Staining signal was visualized using the Vectorstain Elite kit (Vector Laboratories).

X-ray computed tomography. *K19-Nog/C2mE* mice were subjected to X-ray computed tomography using LaTheta LCT-100 (Aloka). Computed tomography analyses were performed 1 wk before celecoxib treatment and at 0, 1, 2, and 3 wk after treatment. Tumor size on computed tomography images was measured using NIH Image software (NIH).

Immunoblotting. Tissue samples were homogenized in lysis buffer. Protein samples were separated in a SDS-polyacrylamide gel. Antibody for the active β-catenin (Upstate) was used. The enhanced chemiluminescence detection system (Amersham) was used to detect specific signals.

Microarray analyses. Total RNA were prepared from mouse stomach at age 30 wk. Expression profiles of the Wnt target genes,[4] cytokines, and chemokines were examined with the Affymetrix GeneChip system and Mouse Genome 430 2.0 Arrays (Affymetrix).

Statistical analyses. Statistical analyses were carried out using Student's *t* test.

Results and Discussion

Generation of *K19-Nog* transgenic mice. To suppress BMP signaling in the stomach, we constructed *K19-Nog* mice that expressed *Nog* encoding noggin in gastric epithelial cells (Fig. 1*A*). Noggin is a polypeptide that inhibits BMP signaling by binding BMP ligands (4). We confirmed increased levels of *Nog* mRNA in *K19-Nog* mouse stomach compared with that in the wild-type by real-time RT-PCR (Fig. 1*B*). BMP type I receptor phosphorylates Smad1,5,8 upon complex formation with BMP ligand and type II receptor (3). We found phosphorylated Smad1,5,8 by immunohistochemistry in the nuclei of differentiated epithelial cells both at the surface and bottom of the gastric gland (Fig. 1*C*), which is consistent with a previous report (11). Notably, in the *K19-Nog* mice, the immunostaining signals of phosphorylated Smad1,5,8 decreased significantly in the upper gastric gland where the K19 promoter is transcriptionally active (Fig. 1*C* and *D*). These results indicate that exogenous *Nog* expression inhibits BMP signaling in the stomach.

Construction of compound mutant mice. We previously constructed *K19-C2mE* transgenic mice expressing both *Ptgs2* and *Ptges* encoding COX-2 and mPGES-1, respectively, in gastric mucosa (Fig. 1*A* and *D*). Expression of COX-2 and mPGES-1 leads to increase of PGE_2 level in *K19-C2mE* mouse stomach (16). To investigate the effect of the PGE_2 pathway in BMP-suppressed gastric mucosa, we crossed *K19-Nog* and *K19-C2mE* mice to generate *K19-Nog/C2mE* compound mice. We confirmed expression of *Ptgs2* by real-time RT-PCR in the stomach of *K19-C2mE* and *K19-Nog/C2mE* mice but not in wild-type and *K19-Nog* mice (Fig. 1*B*). We also used *K19-Wnt1/C2mE* mice for this

[4] http://www.stanford.edu/~rnusse/wntwindow.html

study that develop gastric adenocarcinoma caused by simultaneous activation of the Wnt and PGE_2 pathways (17). Genotypes of respective transgenic strains were confirmed by genomic PCR (Supplementary Fig. S1).

Gastric tumor development in *K19-Nog/C2mE* mice. *K19-Nog* mice did not develop tumorous lesions in the stomach, and the histology of gastric glands was normal (Supplementary Fig. S2; Fig. 2*A*). In contrast, *K19-C2mE* mice developed inflammation-associated hyperplasia, and *K19-Wnt1* mice developed dysplastic preneoplastic lesions, which were consistent with previous reports (16, 17). Importantly, *K19-Nog/C2mE* mice develop large tumors in the glandular stomach (Supplementary Fig. S2; Fig. 2*A*). These results suggest that suppression of BMP signaling is insufficient for gastric tumorigenesis, but that cooperation of BMP inhibition and PGE_2 induction cause gastric tumor development. Such an effect of PGE_2 on tumorigenesis was similar to that found in *K19-Wnt1/C2mE* mice. Activation of Wnt/β-catenin alone leads to development of small preneoplastic lesions, whereas simultaneous activation of the Wnt/β-catenin and PGE_2 pathways cause gastric adenocarcinoma (Fig. 2*A*; ref. 17). Therefore, PGE_2 plays an important role in tumorigenesis regardless of the types of genetic alterations.

JP-type hamartoma in *K19-Nog/C2mE* mouse stomach. Histologically, gastric tumors in *K19-Nog/C2mE* mice displayed irregular branching of epithelial cell layers, combined with dilated cysts that were filled with mucin (Fig. 2*B* and *C*). Such histological characteristics were different from dysplastic tumors of the *K19-Wnt1/C2mE* mice (Fig. 2*B*; ref. 17). We also found abundant α-smooth muscle actin–positive myofibroblasts in stroma. Moreover, we detected infiltration of F4/80-positive macrophages and the accumulation of lymphocytes in the *K19-Nog/C2mE* tumors (Fig. 2*C*). These histological characteristics are typical of the hamartoma of JP patients (9, 10, 18), indicating that suppression of BMP signaling associated with PGE_2 induction causes development of JP-type gastric hamartoma. However, tumor incidence in *K19-Nog/C2mE* mice was 23%, whereas that in *K19-Wnt1/C2mE* mice was 100% (Supplementary Table). Notably, expression of inflammatory cytokine tumor necrosis factor-α (TNF-α) increased in *K19-Nog/C2mE* hamartomas as well as in *K19-C2mE* hyperplasia (Supplementary Fig. S3). However, TNF-α was not induced in nontumor stomach of *K19-Nog/C2mE* mice, whereas transgenic expression of *Ptgs2* stayed at the same level as that in tumor tissues. These results suggest that inflammatory response is also important for hamartoma development together with BMP suppression and PGE_2 induction.

Suppression of gastric hamartoma by COX-2 inhibition. To investigate whether the PGE_2 pathway is required for gastric hamartoma development, we treated *K19-Nog/C2mE* mice with a COX-2 selective inhibitor, celecoxib, at 100 mg/kg/day for 3 weeks. We examined gastric tumor size by X-ray computed tomography scanning, and found that the tumor volume of *K19-Nog/C2mE* mice decreased significantly by celecoxib treatment (Fig. 3*A*). The mean relative tumor size on computed tomography images reduced to 58% after celecoxib treatment (Fig. 3*B*). Histologically, cystic structures were no longer found, and necrotic area was detected in the celecoxib-treated *K19-Nog/C2mE* tumors (Fig. 3*C*). The PGE_2 pathway is important for angiogenesis of gastrointestinal tumorigenesis (15, 19). Consistently, the number of capillary vessels decreased significantly in celecoxib-treated *K19-Nog/C2mE* tumors

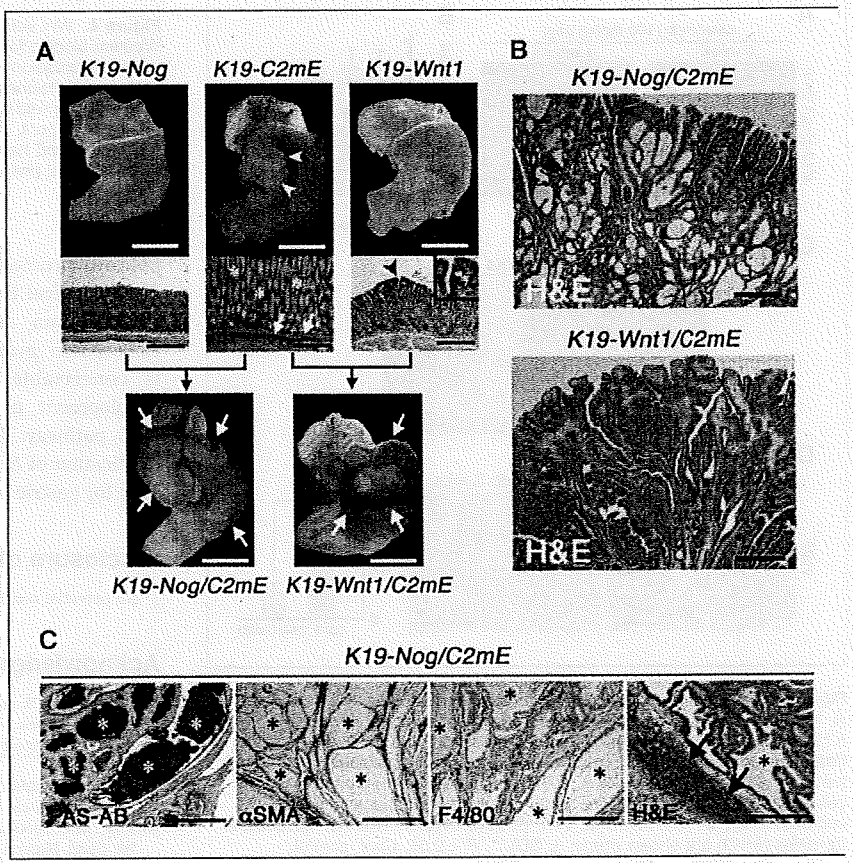

Figure 2. Gastric tumors developed in *K19-Nog/C2mE* mice. *A*, macroscopic photographs and H&E of *K19-Nog*, *K19-C2mE*, and *K19-Wnt1* mouse stomach (*top*). Arrowheads and asterisks in *K19-C2mE* indicate hyperplasia; *arrows*, inflammatory infiltration. Arrowhead and inset in *K19-Wnt1* indicate preneoplastic lesion. Gastric tumors in *K19-Nog/C2mE* and *K19-Wnt1/C2mE* mice are shown (*arrows*, *bottom*). *Bars*, 10 mm. *B*, histology of gastric tumors of *K19-Nog/C2mE* and *K19-Wnt1/C2mE* (H&E). *Bars*, 200 μm. *C*, PAS-Alcian blue, immunostaining for αSMA, F4/80, and H&E of *K19-Nog/C2mE* hamartomas (from left to right). *, dilated cysts. *Arrows*, lymphocyte accumulation. *Bars*, 100 μm.

(Fig. 3*D*). Accordingly, it is possible that angiogenesis is one of the important functions of PGE_2 for hamartoma development.

Wnt-independent development of gastric hamartoma. In the intestinal crypt, inhibition of BMP signaling results in activation of the Wnt/β-catenin pathway (7). We thus examined activation of Wnt signaling in *K19-Nog/C2mE* gastric tumors. The level of the active β-catenin did not increase in *K19-Nog/C2mE* hamartomas, whereas it elevated markedly in *K19-Wnt1/C2mE* tumors (Fig. 4*A*). Consistently, expression of Wnt target genes in *K19-Nog/C2mE* tumors stayed at the same level as that in wild-type mouse stomach, whereas these genes were up-regulated in *K19-Wnt1/C2mE* tumors (Fig. 4*B*). We confirmed that inflammatory cytokines and chemokines were induced in both *K19-Nog/C2mE* and *K19-Wnt1/C2mE* tumors. Accordingly, activation of Wnt signaling is not involved in hamartoma development in BMP-suppressed gastric mucosa, although PGE_2 signaling or PGE_2-dependent inflammation may be required for both adenocarcinoma and hamartoma.

We next examined expression of PGE_2 receptors, EP1 to EP4, in tumor tissues. Notably, the expression of *Ptger1, Ptger2,* and *Ptger3* encoding EP1, EP2, and EP3, respectively, decreased significantly in tumors of *K19-Nog/C2mE* and *K19-Wnt1/C2mE* mice (Fig. 4*C*). In contrast, expression of *Ptger4* encoding EP4 increased dramatically in both *K19-Nog/C2mE* hamartomas and *K19-Wnt1/C2mE* adenocarcinomas. These results suggest that PGE_2 signaling through EP4 is important for development of both gastric hamartoma and adenocarcinoma. Namely, it is possible that the type of genetic alterations determines the histological phenotype of tumors, hamartoma or adenocarcinoma, and that the induced PGE_2 pathway promotes tumor growth through EP4 receptor regardless of histological types (Supplementary Fig. S4).

In human stomach, expression of COX-2 is induced in *Helicobacter pylori*–associated gastric lesions (20). Accordingly, it is conceivable that *H. pylori* infection contributes to the development of gastric hamartoma through induction of the PGE_2 pathway. Therefore, inhibition of the PGE_2 pathway as well as eradication of *H. pylori* may be an effective preventive strategy not only for gastric cancer but also for gastric hamartoma.

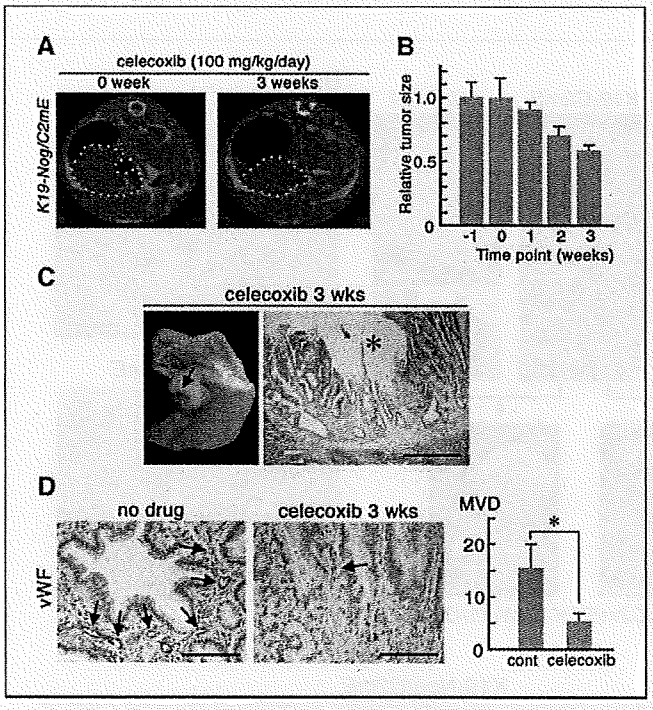

Figure 3. Suppression of hamartoma development by COX-2 inhibition. *A,* X-ray computed tomography images of gastric tumors of the same *K19-Nog/C2mE* mouse (*yellow dashed lines*) at 0 and 3 wk of celecoxib treatment. *B,* relative tumor size at each time point of celecoxib treatment to the level at 0 wk (mean ± SD). *C,* representative photograph and H&E of celecoxib-treated *K19-Nog/C2mE* tumors. *Arrow* and *, necrotic area. *D,* immunostaining for vWF. *Arrows,* vWF-positive capillary vessels. Microvessel densities (*MVD*) are shown (mean ± SD). *, $P < 0.05$. *Cont,* control.

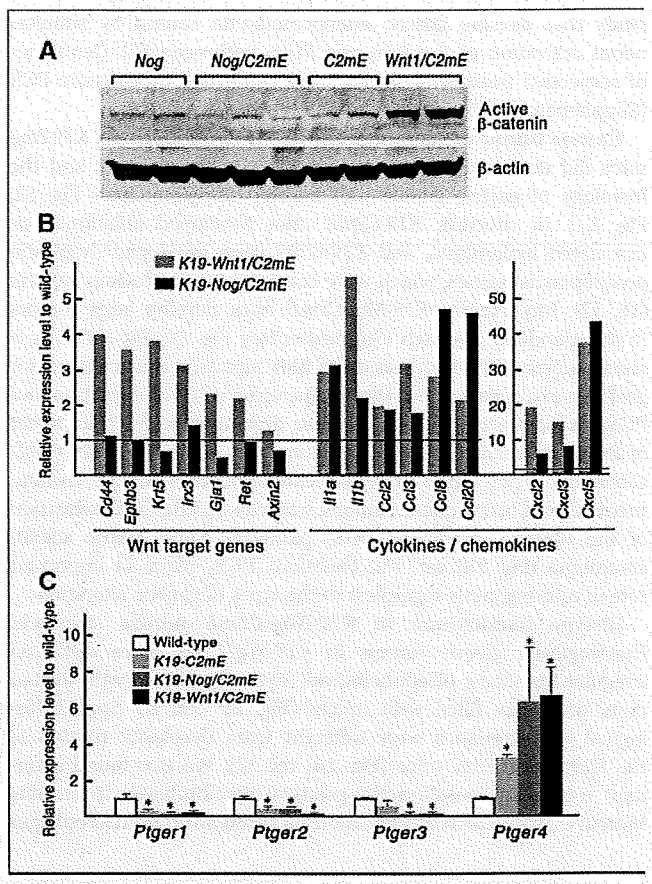

Figure 4. Wnt activity and EP expression in gastric hamartomas. *A,* Western blotting for active β-catenin in the stomach of each genotype. *B,* relative expression levels determined by microarray analyses of Wnt target genes and cytokines/chemokines in *K19-Wnt1/C2mE* and *K19-Nog/C2mE* tumors to the wild-type level. *C,* relative expression levels of PGE_2 receptors, *Ptger1, Ptger2, Ptger3,* and *Ptger4* in *K19-C2mE* hyperplasia, *K19-Nog/C2mE* hamartoma, and *K19-Wnt1/C2mE* adenocarcinoma to the wild-type level (mean ± SD). *, $P < 0.05$.

Disclosure of Potential Conflicts of Interest

No potential conflicts of interest were disclosed.

Acknowledgments

Received 11/18/08; revised 1/13/09; accepted 2/17/09; published OnlineFirst 3/24/09.

Grant support: Grants-in-Aid from the Ministry of Education, Culture, Sports, Science and Technology of Japan, and from the Ministry of Health, Labour and Welfare of Japan.

The costs of publication of this article were defrayed in part by the payment of page charges. This article must therefore be hereby marked *advertisement* in accordance with 18 U.S.C. Section 1734 solely to indicate this fact.

We thank Manami Watanabe for excellent technical assistance.

References

1. Entius MM, Westerman AM, van Velthuysen ML, et al. Molecular and phenotypic markers of hamartomatous polyposis syndromes in the gastrointestinal tract. Hepatogastroenterology 1999;46:661–6.
2. Howe JR, Bair JL, Sayed MG, et al. Germline mutations of the gene encoding bone morphogenetic protein receptor 1A in juvenile polyposis. Nat Genet 2001;28:184–7.
3. Miyazono K, Maeda S, Imamura T. BMP receptor signaling: Transcriptional targets, regulation of signals, and signaling cross-talk. Cytokine Growth Factor Rev 2005;16:251–63.
4. Chen D, Zhao M, Mundy GR. Bone morphogenetic proteins. Growth Factors 2004;22:233–41.
5. Hardwick JCH, van den Brink GR, Bleuming SA, et al. Bone morphogenetic protein 2 is expressed by, and acts upon, mature epithelial cells in the colon. Gastroenterology 2004;126:111–21.
6. Haramis A-PG, Begthel H, van den Born M, et al. Be novo crypt formation and juvenile polyposis on BMP inhibition in mouse intestine. Science 2004;303:1684–6.
7. He XC, Zhang J, Tong W-G, et al. BMP signaling inhibits intestinal stem cell self-renewal through suppression of Wnt-β-catenin signaling. Nat Genet 2004;36:1117–21.
8. Auclair BA, Benoit YD, Rivard N, Mishina Y, Perreault N. Bone morphogenetic protein signaling is essential for terminal differentiation of the intestinal secretory cell lineage. Gastroenterology 2007;133:887–96.
9. Chow E, Macrae F. Review of juvenile polyposis syndrome. J Gastroenterol Hepatol 2005;20:1634–40.
10. Schreibman IR, Baker M, Amos C, McGarrity TJ. The hamartomatous polyposis syndromes: A clinical and molecular review. Am J Gastroenterol 2005;100:476–90.
11. Bleuming SA, He XC, Kodach LL, et al. Bone morphogenetic protein signaling suppresses tumorigenesis at gastric epithelial transition zone in mice. Cancer Res 2007;67:8149–55.
12. Takeda H, Miyoshi H, Tamai Y, Oshima M, Taketo MM. Simultaneous expression of COX-2 and mPGES-1 in mouse gastrointestinal hamartomas. Br J Cancer 2004;90:701–4.
13. Murakami M, Naraba H, Tanioka T, et al. Regulation of prostaglandin E_2 biosynthesis by inducible membrane-associated prostaglandin E_2 synthase that acts in concert with cyclooxygenase-2. J Biol Chem 2000;275:32783–92.
14. Oshima M, Dinchuk JE, Kargman SL, et al. Suppression of intestinal polyposis in $Apc^{\Delta 716}$ knockout mice by inhibition of cyclooxygenase 2 (COX-2). Cell 1996;87:803–9.
15. Sonoshita M, Takaku K, Sasaki N, et al. Acceleration of intestinal polyposis through prostaglandin receptor EP2 in $Apc^{\Delta 716}$ knockout mice. Nat Med 2001;7:1048–51.
16. Oshima H, Oshima M, Inaba K, Taketo MM. Hyperplastic gastric tumors induced by activated macrophages in COX-2/mPGES-1 transgenic mice. EMBO J 2004;23:1669–78.
17. Oshima H, Matsunaga A, Fujimura T, Tsukamoto T, Taketo MM, Oshima M. Carcinogenesis in mouse stomach by simultaneous activation of the Wnt signaling and prostaglandin E_2 pathway. Gastroenterology 2006;131:1086–95.
18. Covarrubias DJ, Huprich JE. Best cases from the AFIP. Juvenile polyposis of the stomach. Radiographics 2002;22:415–20.
19. Guo X, Oshima H, Taketo MM, Oshima M. Stromal fibroblasts activated by tumor cells promote angiogenesis in mouse gastric cancer. J Biol Chem 2008;283:19864–71.
20. Sung JJY, Leung WK, Go MYY, et al. Cyclooxygenase-2 expression in *Helicobacter pylori*-associated premalignant and malignant gastric lesions. Am J Pathol 2000;157:729–35.

Cancer Science
The official journal of the Japanese Cancer Association JCA

Review Article

Prostaglandin E_2, Wnt, and BMP in gastric tumor mouse models

Hiroko Oshima, Keisuke Oguma, Yu-Chen Du and Masanobu Oshima[1]

Division of Genetics, Cancer Research Institute, Kanazawa University, Takara-machi, Kanazawa, Japan

(Received May 26, 2009/Revised June 13, 2009/Accepted June 15, 2009/Online publication July 20, 2009)

The development of gastric cancer is closely associated with *Helicobacter pylori* (*H. pylori*) infection. The expression of cylooxigenase-2 (COX-2), a rate-limiting enzyme for prostaglandin biosynthesis, is induced in *H. pylori*-associated chronic gastritis, which thus results in the induction of proinflammatory prostaglandin, PGE_2. The COX-2/PGE_2 pathway plays a key role in gastric tumorigenesis. On the other hand, several oncogenic pathways have been shown to trigger gastric tumorigenesis. The activation of Wnt/β-catenin signaling is found in 30–50% of gastric cancers, thus suggesting that Wnt signaling plays a causal role in gastric cancer development. Mutations in the bone morphogenetic protein (BMP) signaling pathway are responsible for the subset of juvenile polyposis syndrome (JPS) that develops hamartomas in the gastrointestinal tract. BMP suppression appears to contribute to gastric cancer development because gastric cancer risk is increased in JPS. Wnt signaling is important for the maintenance of gastrointestinal stem cells, while BMP promotes epithelial cell differentiation. Accordingly, it is possible that both Wnt activation and BMP suppression can cause gastric tumorigenesis through enhancement of the undifferentiated status of epithelial cells. Recent mouse model studies have indicated that induction of the PGE_2 pathway is required for the development of both gastric adenocarcinoma and hamartoma in the Wnt-activated and BMP-suppressed gastric mucosa, respectively. This article reviews the involvement of the PGE_2, Wnt, and BMP pathways in the development of gastric cancer, and gastric phenotypes that are found in transgenic mouse models of PGE_2 induction, Wnt activation, BMP suppression, or a combination of these pathways. (*Cancer Sci* 2009; 100: 1779–1785)

Epidemiological studies indicate that the regular use of nonsteroidal anti-inflammatory drugs (NSAIDs) lowers the mortality rate of gastrointestinal cancer.[1] The major target of NSAIDs is cyclooxygenases (COXs), COX-1 and COX-2, which are rate-limiting enzymes for prostaglandin biosynthesis (Fig. 1). COX-1 is constitutively expressed in most tissues and it is considered to be responsible for physiological levels of prostaglandin.[2] In contrast, COX-2 is induced in inflammation by various stimuli including cytokines and growth factors.[3–5] The induction of COX-2 expression is also found in a variety of cancer tissues. Mouse genetic studies have demonstrated that disruption of the *Ptgs2* gene encoding COX-2 results in the suppression of tumor development in the intestine and skin.[6,7] Moreover, various animal studies have confirmed that treatment with NSAIDs or COX-2 selective inhibitors (COXIBs) suppressed chemically induced tumor formation and xenografted tumor growth.[8] These results, taken together, indicate that the COX-2 pathway plays an essential role in cancer development.

However, the mechanism of the COX-2 pathway underlying gastric tumorigenesis has not yet been fully elucidated. To investigate the possible crosstalk between the COX-2 pathway and oncogenic activation in gastric carcinogenesis, a series of mouse models have been constructed and examined as discussed in this review.

Induction of the COX-2/PGE_2 pathway in gastric cancer

Regular use of NSAIDs is associated with a decreased incidence of gastric cancer.[9–12] Induction of COX-2 is found in approximately 70% of gastric cancer, whereas the expression of COX-1 is not elevated.[13,14] Gastric cancer can be divided into two histological subtypes: intestinal and diffuse types, and the expression of COX-2 is found predominantly in the intestinal-type gastric cancer.[15] These results suggest that the COX-2 pathway plays a role in the development of intestinal-type gastric cancer.

Infection with *Helicobacter pylori* (*H. pylori*) causes chronic gastritis, which is associated with gastric carcinogenesis.[16] The expression of COX-2 is significantly induced in the *H. pylori*-infected gastric mucosa, and that COX-2 expression is suppressed by the eradication of *H. pylori*.[17] Although the molecular mechanism for COX-2 induction in tumors has not been elucidated, it is possible that the cytokine network is activated by infection and induces the expression of COX-2. *H. pylori* can stimulate Toll-like receptors (TLRs), leading to activation of the nuclear factor-κB (NF-κB) pathway that induces the expression of COX-2 (Fig. 1).[18,19] Moreover, TLR2/TLR9 signaling by *H. pylori* activates mitogen activated protein kinases (MAPK) including p38, resulting in the activation of CRE and AP-1 elements on the COX-2 gene promoter.[19,20]

Microsomal PGE synthase-1 (mPGES-1), a PGE_2 converting enzyme is functionally coupled with COX-2.[21] Simultaneous induction of COX-2 and mPGES-1 is observed in gastric cancer tissues suggesting induction of the PGE_2 pathway in gastric tumors (Fig. 1).[22,23] The level of mPGES-1 also decreases after the eradication of *H. pylori*,[24] thus indicating that *H. pylori* infection induces the PGE_2 pathway through induction of both COX-2 and mPGES-1. The PGE_2 level significantly increases in gastric cancer,[25] and the level is associated with the *H. pylori* infection status.[26]

Gastric tumor development in mouse and rat models induced by chemical carcinogens or *Helicobacter* infection is suppressed by treatment with NSAIDs or COXIBs.[27–29] *H. pylori* infection in Mongolian gerbils induces gastric tumorigenesis, which is quite similar to the course of human gastric carcinogenesis. Importantly, treatment with *H. pylori*-infected and chemical carcinogen-treated Mongolian gerbils with a COXIB suppressed gastric carcinogenesis.[30,31] These animal studies suggest that the COX-2 pathway thus plays an essential role in *H. pylori* infection–associated gastric tumorigenesis.

[1]To whom correspondence should be addressed.
E-mail: oshimam@kenroku.kanazawa-u.ac.jp

doi: 10.1111/j.1349-7006.2009.01258.x